Dynamic Event-Triggered Control of Linear Continuous-Time Systems using a Positive Systems Approach

Safeyya Alyahia, Corina Barbalata, Michael Malisoff, Frédéric Mazenc

Dynamic Event-Triggered Control of Linear Continuous-Time Systems using a Positive Systems Approach*

Safeyya Alyahia† Corina Barbalata‡ Michael Malisoff† Frédéric Mazenc§

April 13, 2024

Abstract

We provide new dynamic event-triggered controls for continuous-time linear systems that contain additive uncertainties. We prove input-to-state stability properties that imply uniform global exponential stability when the additive uncertainties are zero. Significant novel features include (a) new dynamic extensions and new trigger rules that provide a new positive systems analog of significant prior dynamic event-triggered work of A. Girard and (b) our application to a BlueROV2 underwater vehicle model, where we provide significantly larger lower bounds on the inter-execution times, and usefully fewer trigger times, compared with standard dynamic event-triggered approaches that used the usual Euclidean norm, and as compared with static event-triggered controls that instead used positive systems approaches.

1 Introduction

Event-triggered control is an alternative to more well-known standard control methods, where instead of changing control values at times that are independent of the state, the times when the event-triggered control values change depend on the state or output. This calls for finding (a) the control, whose values only change at event triggering times and (b) a trigger rule, to choose event triggering times; see [1, 2]. This can help reduce the use of scarce communication resources, by only changing control values when the system requires attention. This led to a large theoretic literature on event-triggered control and widespread use of event-triggered controls, especially in communication networks [3, 4, 5, 6, 7, 8, 9, 10, 11, 12, 13, 14, 15, 16, 17, 18, 19].

This paper continues our development (begun in [20, 21, 22, 23, 24]) of event-triggered control methods that can help overcome important challenges in feedback control, such as reducing the number of instants when controls change values on given time intervals as compared with standard controls, ensuring robustness to model uncertainty, and eliminating the need to continuously measure state or output values. While our preceding works were confined to static event triggers, here we consider higher dimensional dynamic event triggers, which interconnect the given system with an additional dynamical system, leading to very different triggering criteria. Our work is strongly motivated by notable theoretical results (such as [25, 26]) and applications (such as [27]) that demonstrated potential advantages of dynamic event triggers over static ones, e.g., in terms of increasing the lower bound on the inter-execution times (which are the lengths of time between consecutive event triggering times) or improving the performance of communication networks.

In [20, 21, 22, 23, 24], key ingredients in our analysis of the static triggering case were interval observers (which are also called comparison systems), a positive systems approach, and replacing the usual Euclidean norm (or the corresponding induced matrix operator norm) by matrices of absolute values. These works

*Supported by the US National Science Foundation under Grant 2009659. Key Words: dynamic extension, triggered control

†S. Alyahia and M. Malisoff are with Department of Mathematics, 303 Lockett Hall, 175 Field House Drive, Louisiana State University, Baton Rouge, LA 70803, USA (e-mails: salyah2@lsu.edu, malisoff@lsu.edu).

‡C. Barbalata is with Department of Mechanical and Industrial Engineering, 3261 Patrick F. Taylor Hall, Louisiana State University, Baton Rouge, LA 70803, USA (e-mail: cbarbalata@lsu.edu).

§F. Mazenc is with INRIA EPI DISCO, L2S-CNRS-CentraleSupélec, 3 rue Joliot Curie, 91192, Gif-sur-Yvette, France (e-mail: frederic.mazenc@centralesupelec.fr).

illustrated the main advantages of using matrices or vectors of absolute values instead of the usual Euclidean norm, which were (a) a significant reduction in the number of trigger times on given time intervals that is made possible by using the entrywise absolute values and (b) the fact that this replacement did not degrade other performance metrics in terms of overshoots, transient behavior, and undershoots, when applied to the BlueROV2 vehicle, which is commonly used and plays a vital role in ecological robotics to study corals. Although we do not require our given systems to satisfy positivity conditions, our interval observers produce positive dynamics for $(\overline{x}, -\underline{x})$ and $(\overline{x} - x, x - \underline{x})$, where $\overline{x}$ and $\underline{x}$ are the upper and lower bounding functions in the interval observer for the closed loop system state x, respectively, so they satisfy the framing condition $\underline{x}(t) \leq x(t) \leq \overline{x}(t)$ for all $t \geq 0$. Interval observers appeared, e.g., in [28], leading to solutions of stabilization problems. However, we believe that the work in this paper is the first to apply this approach in the context of dynamic event-triggered control, using our new dynamical extensions that define the feedback control values and new triggering rules that we present below which have not appeared before. Hence, this paper provides an approach that is not overlapping with any previous dynamic event-triggered works, e.g., [29, 30].

In Section 2, we present our dynamic event-triggered results using sampled state values, and Section 3 provides an analog with outputs. Another significantly novel ingredient is a variant of the continuous-discrete observer from [31]. While [31] did not cover event-triggering, our method for finding a positive lower bound on the inter-execution times (and so ruling out the Zeno phenomenon, which would have allowed an infeasible infinite number of trigger times on some interval of finite length), combined with our mild upper bound on these lengths, allow us to satisfy the uniform observability requirement from [31]. In Section 4, we discuss criteria for comparing the performances of event-triggered controls. In Section 5, we apply our new approaches to a model of the BlueROV2 vehicle. Significantly novel features are then (a) our new dynamic extensions and new trigger rules that provide a positive systems analog of significant dynamic event-triggered control work of A. Girard and (b) our application to a BlueROV2 underwater vehicle model, where our method provides significantly larger lower bounds on the inter-execution times, and fewer trigger times on given intervals, compared with standard dynamic event-triggered approaches that used the usual Euclidean norm, and compared with prior static event-triggered controls such as [20] that instead used positive systems approaches (using two criteria from Section 4), without significant degradation of settling times, overshoots, or undershoots. Unlike [26], we only consider linear systems, and do not include delays, but we establish input-to-state stability (ISS) under additive disturbances; see [32, 33] for the standard definitions for ISS.

We use this other notation. The dimensions of our Euclidean spaces are arbitrary, unless we indicate otherwise. For any function f defined on an interval $\mathcal{I}$, $f(t^-)$ is its left limit at points t in the closure of $\mathcal{I}$. Set $\mathbb{Z}_0 = \{0, 1, 2, ...\}$ and $\mathbb{N} = \mathbb{Z}_0 \setminus \{0\}$. For a matrix $G = [g_{ij}] \in \mathbb{R}^{r \times s}$, set $|G| = [|g_{ij}|]$, so the entries of $|G|$ are absolute values of the corresponding entries g_{ij} of G. By G^+, we denote the matrix whose entry in row i and column j is $\max\{0, g_{ij}\}$ for all i and j, and $G^- = G^+ - G$. Then $|G| = G^+ + G^-$. A square matrix is called Schur stable provided its spectral radius is in $[0, 1)$, $||\cdot||$ denotes the usual Euclidean norm and corresponding operator matrix norm, $||f||_{\mathcal{I}}$ is the supremum of functions f in this norm over a subset $\mathcal{I}$ of their domains, I is the identity matrix, and 0 is the zero matrix. When $f = [f_{ij}]$ is matrix valued, we set $\sup_{\ell \in \mathcal{I}} |f(\ell)| = [h_{ij}]$ (which we also denote by $|f|_{\mathcal{I}}$) where $h_{ij} = \sup_{\ell \in \mathcal{I}} |f_{ij}(\ell)|$ for all i and j when these suprema are finite. For matrices $D = [d_{ij}]$ and $E = [e_{ij}]$ of the same size, we write $D < E$ (resp., $D \leq E$) provided $d_{ij} < e_{ij}$ (resp., $d_{ij} \leq e_{ij}$) for all i and j. We adopt similar notation for vectors. A matrix S is called positive provided $0 < S$. For $M \in \mathbb{R}^{n \times n}$, D_M is the diagonal matrix whose main diagonal entries agree with those of M, $R_M = D_M + (M - D_M)^+$ and $N_M = (M - D_M)^+ - (M - D_M)$, so $M = R_M - N_M$. Also, $M_1 \preceq M_2$ for square matrices M_1 and M_2 of the same size means that $M_2 - M_1$ is nonnegative definite. Hence, we use $\preceq$ instead of $\leq$, to denote the nonnegative definiteness condition, to avoid confusion with the entrywise inequalities $\leq$ of entries of matrices. We also let $\mathbf{1}_n \in \mathbb{R}^n$ denote the vector whose entries are all 1's. Finally, we say that a real square matrix is Metzler (resp., Hurwitz) provided all of its off-diagonal elements are nonnegative (resp., all of its eigenvalues have negative real parts).

2 State Feedback Result

2.1 Studied system

We consider the system

$$\dot{x}(t) = Ax(t) + Bu(t) + \delta(t) \tag{1}$$

where x is valued in $\mathbb{R}^n$, the control u is valued in $\mathbb{R}^p$ and will be specified below, A and B are known real matrices, and $\delta : [0, +\infty) \to \mathbb{R}^n$ is piecewise continuous [32] but unknown (but see Section 3 for analogs for systems with outputs). We introduce two assumptions, the first of which is a positive systems analog of controllability (as noted in [20]) and uses the R_M and N_M notation as reviewed in Section 1 above in the special case where the M from Section 1 is $M = H$, and the second of which is generally satisfied because bounds on uncertainties are usually known. See also Remark 3.1 below, for motivation for our assumptions.

Assumption 1 *There is a matrix $K \in \mathbb{R}^{p\times n}$ such that with the choice $H = A + BK$, the matrix $R_H + N_H$ is Hurwitz.*

Assumption 2 *There is a known continuous function $\Delta : [0, +\infty) \to [0, +\infty)^n$ such that*

$$|\delta(t)| \leq \Delta(t) \tag{2}$$

for all $t \geq 0$.

Assumption 1 ensures that there are a vector $V > 0$ in $\mathbb{R}^n$ and a constant $c > 0$ such that

$$V^\top (R_H + N_H) \leq -cV^\top, \tag{3}$$

since $R_H + N_H$ is Metzler and Hurwitz; see [34, Theorem 2.11, p. 38]. We fix V, K, and c satisfying the preceding requirements in what follows. Let $\Gamma > 0$ be a matrix in $\mathbb{R}^{n\times n}$ such that there is a constant $r > 0$ such that

$$-cV^\top + V^\top |BK|\Gamma \leq -rV^\top, \tag{4}$$

which will hold when all entries of Γ are small enough positive values. We will also use the function

$$\Omega(s) = e^{As} + \textstyle\int_0^s e^{mA}\mathrm{d}mBK. \tag{5}$$

Since $\Gamma > 0$ and $\Omega(0) = I$, there is a constant $\nu > 0$ such that $\Omega(t)$ is nonsingular for each $t \in [0, \nu]$ and such that

$$|\Omega^{-1}(s) - I| \leq \Gamma \ \text{ for all } \ s \in [0, \nu]. \tag{6}$$

We fix c, r, A, B, V, Δ, Γ, K, and ν satisfying the preceding requirements in the sequel.

2.2 Triggered control

We turn next to our dynamic event-triggered control, in the special case where sampled state measurements from the system are available. It is composed of (a) the closed loop system, which uses the control gain K that we introduced in Assumption 1 above, (b) a dynamic extension that is computed using the sampled state measurements, and (c) a trigger rule that uses our bounding function Δ from Assumption 2 and so does not require knowing values $\delta(t)$ of the uncertainty δ in (1). This leads to an asymptotic stability proof, which uses the interval observer ideas that we introduced above in the introduction.

To provide the required formulas for our event-triggered control in this case, we first fix a diagonal matrix $D \in \mathbb{R}^{n\times n}$ whose main diagonal entries are all positive, which is a tuning matrix, any positive vector $z_0 \in \mathbb{R}^n$, and any constant $T > \nu$. Consider

$$\left\{\begin{array}{rcl} \dot{x}(t) &=& Ax(t) + BKx(\sigma(t)) + \delta(t) \ \text{ for all } \ t \geq 0 \\ \dot{w}(t) &=& Aw(t) + BKx(t_i) \ \text{ for all } \ t \in [t_i, t_{i+1}) \ \text{ and } \ w(t_i) = x(t_i) \ \text{ for all } \ i \in \mathbb{Z}_0 \\ \dot{z}(t) &=& (R_H + N_H)z(t) - |BK|(|e(t)| - \Gamma|w(t)|) + \lambda(\Delta_t) \ \text{ for all } \ t \geq 0, \ \text{ and } \ z(0) = z_0 \\ e(t) &=& x(t_i) - w(t) \ \text{ for all } \ t \in [t_i, t_{i+1}) \ \text{ and } \ i \in \mathbb{Z}_0 \\ t_{i+1} &=& \sup\{t \in [t_i, t_i + T] : z(t) - D|BK|(|e(t)| - \Gamma|w(t)|) + D\lambda(\Delta_t) > 0\} \end{array}\right. \tag{7}$$

where $t_0 = 0$, $\sigma(t) = \max\{t_i : i \geq 0 \ \text{ and } \ t_i \leq t\}$ is the largest trigger time t_i in $[0, t]$ for each $t \geq 0$, and

$$\lambda(\Delta_t) = |BK| \left[\sup_{s\in[0,\nu]} \left|\Omega^{-1}(s)\right| + I + 2\Gamma\right] \textstyle\int_{(t-\nu)^+}^t \left|e^{A(t-\ell)}\right| \Delta(\ell)\mathrm{d}\ell. \tag{8}$$

The main role of λ (and its analogs in our other trigger rules below) is to collect the effects of the uncertainty bounds Δ in the trigger rules and in the dynamic extensions without requiring knowledge of δ. This triggered control mechanism (7) is reminiscent of those of [26], except we adopt a positive systems approach, and we also introduce the w dynamics to eliminate the need for the triggering rule to continuously measure $x(t)$. The implementation of (7) is as follows. The method in (7) calls for using the control $u(t) = Kx(\sigma(t))$, whose values are found in the following recursive way. We solve the initial value problems given by the x, w, and z systems in (7) with the initial time 0 and initial states $x(0)$, $z(0) = z_0$, and $w(0) = x(0)$ respectively, while monitoring the strict inequality in the sup in (7) with $i = 0$. If the strict inequality in the sup is satisfied for all $t \in [0, T]$, then we set $t_1 = T$. Otherwise, this supremum is in $[0, T)$, and is chosen as our first positive trigger time t_1. Then we repeat this process with $t_0 = 0$ replaced by t_1, by solving the initial value problems for the x, w, and z systems in (7) with $i = 1$ and the initial time t_1 and the initial state $z(t_1)$ obtained by having solved the z system in (7) on $[0, t_1]$, and with $x(t_1) = w(t_1) = x(t_1^-)$. This repeats for all $i \in \mathbb{Z}_0$, and gives a continuous solution $x(t)$ for all $t \geq 0$ and the trigger time sequence $\{t_i\}$, because as shown in the second part of the proof of our first theorem, the Zeno phenomenon does not occur. While not explicitly in (7) or in the statement of our first theorem, the positive systems approach is used in the proof, to give the framing property $\underline{x}(t) \leq x(t) \leq \overline{x}(t)$ using the positive dynamics for $(\overline{x}, -\underline{x})$ and for $(\overline{x} - x, x - \underline{x})$, where $\overline{x}$ and $\underline{x}$ comprise the upper and lower bounds in the interval observer, respectively. We prove:

Theorem 1 *Let Assumptions 1-2 hold. Then we can find positive constants c_1 and c_2 such that for all solutions $x : [0, +\infty) \to \mathbb{R}^n$ of (1) with the preceding event-triggered control given by (7) and $u(t) = Kx(\sigma(t))$, we have $||x(t)|| \leq c_1 e^{-rt}||(x(0), z_0)|| + c_2||\Delta||_{[0,t]}$ for all $t \geq 0$. Also, $t_{i+1} - t_i \in [\nu, T]$ for all $i \in \mathbb{Z}_0$.*

In the special case where there is no uncertainty δ in the system, the preceding theorem ensures global exponential convergence of $x(t)$ to the origin, because in that case we can choose Δ to be the zero function.

2.3 Proof of Theorem 1

The proof has four parts. First, we prove that the solution of the z system in (7) with $z(0) = z_0$ satisfies $z(t) > 0$ for all $t \geq 0$. Then, we prove that the Zeno phenomenon does not occur, by showing that $t_{i+1} - t_i \geq \nu$ for all $i \in \mathbb{Z}_0$. In the third part, we build our interval observer, to prove the bound on $||x(t)||$ from the theorem in the fourth part. We use the fact that for each compact interval $\mathcal{I} \in [0, +\infty)$, there is a constant $g > 0$ such that $e^{(R_H + N_H)\ell} \geq gI$ for all $\ell \in \mathcal{I}$. To find g, note that the functions $q_1(t) = e^{(R_H+N_H)t}\mathcal{E}_j$ and $q_2(t) = e^{D_H t}\mathcal{E}_j$ satisfy $q_1(0) = q_2(0)$, $\dot{q}_1(t) - \dot{q}_2(t) = D_H(q_1(t) - q_2(t)) + (R_H + N_H - D_H)q_1(t)$ and so also

$$e^{(R_H+N_H)t}\mathcal{E}_j - e^{D_H t}\mathcal{E}_j = q_1(t) - q_2(t) = \int_0^t e^{D_H(t-\ell)}(R_H + N_H - D_H)q_1(\ell)\mathrm{d}\ell \geq 0 \tag{9}$$

for all $t \geq 0$, and $e^{(R_H+N_H)\ell}\mathcal{E}_j \geq e^{D_H \ell}\mathcal{E}_j$ for $j = 1, \ldots n$ and all $\ell \geq 0$, by the nonnegativity of $R_H + N_H - D_H$ and the fact that $[0, +\infty)^n$ is forwardly invariant for the cooperative system $\dot{q}_1 = (R_H + N_H)q_1$ [31] (so $q_1(t) \geq 0$ for all $t \geq 0$) and applying the method of variation of parameters to the dynamics for $q_1 - q_2$, where $\mathcal{E}_j \in \mathbb{R}^n$ is the jth standard basis vector. This lets us pick $g = \min_{\ell \in \mathcal{I}} \min_i e^{-|d_i \ell|}$, where d_i is the ith diagonal entry of D_H for $i = 1, \ldots, n$.

First Part: Positivity of z. We prove that $z(t) > 0$ for all $t \geq 0$. First, we prove that $z(t) > 0$ for all $t \in [0, t_1)$. We proceed by contradiction. Suppose that there were a $t_c \in [0, t_1)$ such that $z(t) > 0$ for all $t \in [0, t_c)$ and such that there is a $j \in \{1, ..., n\}$ such that $z_j(t_c) = 0$. Since the last inequality in (7) with $i = 0$ gives $z(t) - D|BK|(|e(t)| - \Gamma|w(t)|) + D\lambda(\Delta_t) \geq 0$ for all $t \in [0, t_1)$, the z dynamics in (7) gives

$$\dot{z}(t) \geq (R_H + N_H)z(t) - D^{-1}z(t) \geq (D_H - D^{-1})z(t) \tag{10}$$

for all $t \in [0, t_c]$, since the off-diagonal entries of $R_H + N_H$ are nonnegative and $z(t) \geq 0$ for all $t \in [0, t_c]$. Applying an integrating factor to $\dot{z}(t) \geq (D_H - D^{-1})z(t)$ then gives $z(t) \geq e^{(D_H - D^{-1})t}z(0)$ for all $t \in [0, t_c]$. Since $z(0) > 0$, and since $D_H + D^{-1}$ is diagonal, it follows that $z(t) > 0$ for all $t \in [0, t_c]$, contradicting the definition of t_c. Hence, by induction, $z(t) > 0$ for all $t \in [t_i, t_{i+1})$ and all i.

Second Part: Ruling out Zeno's phenomenon. To prove that Zeno's phenomenon does not occur, first fix an $i \in \mathbb{Z}_0$. By applying the method of variation of parameters to the x dynamics in (7), we get

$$x(t) = \Omega(t - t_i)x(t_i) + \int_{t_i}^t e^{A(t-m)}\delta(m)\mathrm{d}m \text{ for all } t \in [t_i, t_{i+1}), \tag{11}$$

where Ω is the function defined in (5). Hence, our choice $e(t) = x(t_i) - w(t)$ from (7) gives

$$[\Omega(t-t_i)^{-1} - I]x(t) = e(t) + \Omega(t-t_i)^{-1}\int_{t_i}^{t} e^{A(t-m)}\delta(m)\mathrm{d}m + w(t) - x(t) \ \text{ for all } \ t \in [t_i, t_{i+1}) \tag{12}$$

if $t_{i+1} - t_i \leq \nu$, by left multiplying (11) through by $\Omega(t-t_i)^{-1}$, then subtracting $x(t)$ from both sides of the result, and then subtracting and adding $w(t)$ on the right side of the result. It follows that

$$|e(t)| \leq \left|\left[\Omega(t-t_i)^{-1} - I\right]x(t) - \Omega(t-t_i)^{-1}\int_{t_i}^{t} e^{A(t-m)}\delta(m)\mathrm{d}m\right| + |w(t) - x(t)| \ \text{ for all } \ t \in [t_i, t_{i+1}) \tag{13}$$

if $t_{i+1} - t_i \leq \nu$, so the relation $-\Gamma|w(t)| \leq -\Gamma|x(t)| + \Gamma|w(t) - x(t)|$ gives

$$\begin{array}{rcl} |e(t)| - \Gamma|w(t)| & \leq & [|\Omega(t-t_i)^{-1} - I| - \Gamma]|x(t)| \\ & & + \left|\Omega(t-t_i)^{-1}\int_{t_i}^{t} e^{A(t-m)}\delta(m)\mathrm{d}m\right| + (I+\Gamma)|w(t) - x(t)| \ \text{ for all } \ t \in [t_i, t_{i+1}) \end{array} \tag{14}$$

if $t_{i+1} - t_i \leq \nu$. Also, (7) gives $\dot{x}(t) - \dot{w}(t) = A(x(t) - w(t)) + \delta(t)$, so we can apply the method of variation of parameters to the dynamics for $x - w$ on the interval $[t_i, t]$ to obtain

$$x(t) - w(t) = \int_{t_i}^{t} e^{A(t-\ell)}\delta(\ell)\mathrm{d}\ell \tag{15}$$

for all $i \in \mathbb{Z}_0$ and $t \in [t_i, t_{i+1})$, because $x(t_i) = w(t_i)$. We next proceed by contradiction. Suppose that $t_{i+1} - t_i < \nu$. Then (6) ensures that $|\Omega^{-1}(t-t_i) - I| \leq \Gamma$ for all $t \in [t_i, t_{i+1})$. Consequently, (14)-(15) give

$$|e(t)| - \Gamma|w(t)| \leq \left|\Omega(t-t_i)^{-1}\int_{t_i}^{t} e^{A(t-m)}\delta(m)\mathrm{d}m\right| + (I+\Gamma)\left|\int_{t_i}^{t} e^{A(t-\ell)}\delta(\ell)\mathrm{d}\ell\right| \ \text{ for all } \ t \in [t_i, t_{i+1}), \tag{16}$$

by using (15) to upper bound the last right side term of (14). Since $|BK| \geq 0$, it follows that

$$-|BK|(|e(t)| - \Gamma|w(t)|) \geq -|BK|\left|\Omega(t-t_i)^{-1}\mathcal{L}(t)\right| - |BK|(I+\Gamma)\left|\mathcal{L}(t)\right| \ \text{ for all } \ t \in [t_i, t_{i+1}), \tag{17}$$

where $\mathcal{L}(t)$ is the integral in (15). Consequently, our formula for the z dynamics in (7) gives

$$\dot{z}(t) \geq (R_H + N_H)z(t) - |BK|\left|\Omega(t-t_i)^{-1}\mathcal{L}(t)\right| - |BK|(I+\Gamma)\left|\mathcal{L}(t)\right| + \lambda(\Delta_t) \ \text{ for all } \ t \in [t_i, t_{i+1}). \tag{18}$$

On the other hand, since $t_{i+1} - t_i < \nu$, it follows from (2) and the definition of $\lambda(\Delta_t)$ in (8) that

$$-|BK|\left|\Omega(t-t_i)^{-1}\mathcal{L}(t)\right| - |BK|(I+2\Gamma)\left|\mathcal{L}(t)\right| + \lambda(\Delta_t) \geq 0 \tag{19}$$

for all $t \in [t_i, t_{i+1})$, so (18) gives $\dot{z}(t) \geq (R_H + N_H)z(t) \geq D_H z(t)$ for all $t \in [t_i, t_{i+1})$, by again using the nonnegativity of the off-diagonal elements of $R_H + N_H$ and the fact that $z(t) \geq 0$ for all $t \geq 0$. Therefore, we can again apply an integrating factor (to the differential inequality (18) for $z(t)$) to obtain

$$z(t) \geq e^{D_H(t-t_i)}z(t_i) \geq \underline{d}z(t_i) \ \text{ for all } \ t \in [t_i, t_{i+1}), \tag{20}$$

where $\underline{d} = \min\{e^{-|d_i|\nu} : 1 \leq i \leq n\}$ where d_i is as defined above. Since $D \geq 0$, (17) and (20) then give

$$z(t) - D|BK|(|e(t)| - \Gamma|w(t)|) + D|BK|\left(\left|\Omega(t-t_i)^{-1}\mathcal{L}(t)\right| + (I+\Gamma)\left|\mathcal{L}(t)\right|\right) \geq \underline{d}z(t_i) \tag{21}$$

for all $t \in [t_i, t_{i+1})$. By left multiplying (19) through by D, we obtain

$$D\lambda(\Delta_t) - D|BK|\Gamma|\mathcal{L}(t)| \geq D|BK||\Omega(t-t_i)^{-1}\mathcal{L}(t)\big| + D|BK|(I+\Gamma)|\mathcal{L}(t). \tag{22}$$

By using (22) to upper bound the last two left side terms in (21), we obtain

$$\begin{array}{l} z(t) - D|BK|(|e(t)| - \Gamma|w(t)|) + D\lambda(\Delta_t) - D|BK|\Gamma|\mathcal{L}(t)| \\ \geq z(t) - D|BK|(|e(t)| - \Gamma|w(t)|) + D|BK|\left(\left|\Omega(t-t_i)^{-1}\mathcal{L}(t)\right| + (I+\Gamma)\left|\mathcal{L}(t)\right|\right) \geq \underline{d}z(t_i). \end{array} \tag{23}$$

Therefore, since $z(t) > 0$ for all $t \geq 0$ and $e(t_{i+1}) = 0$, we get

$$z(t) - D|BK|(|e(t)| - \Gamma|w(t^-)|) + D\lambda(\Delta_t) - D|BK|\Gamma|\mathcal{L}(t)| > 0 \text{ for all } t \in (t_i, t_{i+1}], \tag{24}$$

where the left limit t^- is only needed for (24) to hold at t_{i+1}. On the other hand, since (7) gives $w(t_{i+1}) = x(t_{i+1})$, (15) gives $D|BK|\Gamma|w(t_{i+1}^-)| - D|BK|\Gamma|w(t_{i+1})| \leq D|BK|\Gamma|w(t_{i+1}) - w(t_{i+1}^-)| = D|BK|\Gamma|x(t_{i+1}) - w(t_{i+1}^-)| \leq D|BK|\Gamma|\mathcal{L}(t_{i+1})|$, hence $D|BK|\Gamma|w(t_{i+1}^-)| - D|BK|\Gamma|\mathcal{L}(t_{i+1})| \leq D|BK|\Gamma|w(t_{i+1})|$, so (24) gives

$$z(t) - D|BK|(|e(t)| - \Gamma|w(t)|) + D\lambda(\Delta_t) > 0 \tag{25}$$

for all $t \in [t_i, t_{i+1}]$. Since $z(t)$, $|e(t)|$, $|w(t)|$ and $\lambda(\Delta_t)$ are right continuous, this provides a constant $\epsilon_0 > 0$ such that (25) holds for all $t \in [t_i, t_{i+1} + \epsilon_0]$. This yields a contradiction with the definition of t_{i+1} in (7).

Third Part: Interval observer. We use the interval observer

$$\left\{ \begin{array}{rcl} \dot{\overline{x}}(t) & = & R_H\overline{x}(t) - N_H\underline{x}(t) + (BK(x(\sigma(t)) - x(t)))^+ + \delta(t)^+ \\ \dot{\underline{x}}(t) & = & R_H\underline{x}(t) - N_H\overline{x}(t) - (BK(x(\sigma(t)) - x(t)))^- - \delta(t)^- \end{array} \right. \tag{26}$$

and the facts that the x dynamics can be written as

$$\dot{x}(t) = (R_H - N_H)x(t) + (BK(x(\sigma(t)) - x(t)))^+ - (BK(x(\sigma(t)) - x(t)))^- + \delta(t)^+ - \delta(t)^- \tag{27}$$

for all $t \geq 0$, and that the $2n \times 2n$ matrix $\mathcal{M}$ defined by

$$\mathcal{M} = \left[\begin{array}{cc} R_H & N_H \\ N_H & R_H \end{array} \right] \tag{28}$$

is Metzler, which will be a positive systems approach. To this end, we can combine (26)-(27) to check that the dynamics for the variables $X_a = [\overline{x} - x, x - \underline{x}]^\top$ and $X_b = [\overline{x}, -\underline{x}]^\top$ have the state space $\mathbb{R}^{2n}$ and are defined by

$$\dot{X}_a(t) = \mathcal{M}X_a(t) + \mathcal{N}_a(t) \quad \text{and} \quad \dot{X}_b(t) = \mathcal{M}X_b(t) + \mathcal{N}_b(t) \tag{29}$$

with the choices

$$\mathcal{N}_a(t) = \left[\begin{array}{c} (BK(x(\sigma(t)) - x(t)))^- + \delta(t)^- \\ (BK(x(\sigma(t)) - x(t)))^+ + \delta(t)^+ \end{array} \right] \text{ and } \mathcal{N}_b(t) = \left[\begin{array}{c} (BK(x(\sigma(t)) - x(t)))^+ + \delta(t)^+ \\ (BK(x(\sigma(t)) - x(t)))^- + \delta(t)^- \end{array} \right] \tag{30}$$

for all $t \geq 0$. Since $\mathcal{M}$ is Metzler, and since $\mathcal{N}_a$ and $\mathcal{N}_b$ in (30) are nonnegative matrix valued functions, it follows from properties of cooperative (or positive) systems (e.g., from [31, Lemma 1]) that the dynamics for X_a and X_b in (29) are cooperative, i.e., (i) if $X_a(0) \geq 0$, then $X_a(t) \geq 0$ for all $t \geq 0$ and (ii) if $X_b(0) \geq 0$, then $X_b(t) \geq 0$ for all $t \geq 0$. By separately considering the components of X_a and X_b, it follows that if

$$\overline{x}(0) \geq 0, \ \underline{x}(0) \leq 0, \ \text{ and } \ \underline{x}(0) \leq x(0) \leq \overline{x}(0), \tag{31}$$

then we have

$$\overline{x}(t) \geq 0, \ \underline{x}(t) \leq 0 \ \text{ and } \ \underline{x}(t) \leq x(t) \leq \overline{x}(t) \tag{32}$$

for all $t \geq 0$, e.g., by [31, Lemma 1]. We deduce that $\underline{x}(t) - \overline{x}(t) \leq x(t) \leq \overline{x}(t) - \underline{x}(t)$ and so also

$$|x(t)| \leq \overline{x}(t) - \underline{x}(t) \tag{33}$$

for all $t \geq 0$ if (31) hold.

Fourth Part: Stability analysis. We let (31) hold, and we use the linear Lyapunov function

$$U(\overline{x}, \underline{x}, z) = V^\top(\overline{x} - \underline{x} + z), \tag{34}$$

where $V \in \mathbb{R}^n$ is the positive vector chosen in Section 2.1. Then, using the fact that (26) gives

$$\dot{\overline{x}}(t) - \dot{\underline{x}}(t) = (R_H + N_H)(\overline{x}(t) - \underline{x}(t)) + |BK(x(t_i) - x(t))| + |\delta(t)| \tag{35}$$

for all $t \geq 0$ and the nonnegative valuedness of $\overline{x} - \underline{x}$ (which follows from (32)) and of z (which follows from the first part of the proof), we conclude from (3) that the time derivative of U along the trajectories of (26) and (7) satisfies

$$\begin{array}{rcl} \dot{U}(t) & \leq & -cV^\top(\overline{x}(t) - \underline{x}(t)) + V^\top|BK(x(t_i) - x(t))| - cV^\top z(t) - V^\top|BK|(|e(t)| - \Gamma|w(t)|) \\ & & +V^\top|\delta(t)| + V^\top\lambda(\Delta_t) \\ & \leq & -cV^\top(\overline{x}(t) - \underline{x}(t) + z(t)) + V^\top|BK|\Gamma|x(t)| + V^\top|\delta(t)| \\ & & +V^\top|BK|(I+\Gamma)\left|\int_{\sigma(t)}^t e^{A(t-\ell)}\delta(\ell)\mathrm{d}\ell\right| + V^\top\lambda(\Delta_t) \\ & \leq & -cV^\top(\overline{x}(t) - \underline{x}(t) + z(t)) + V^\top|BK|\Gamma(\overline{x}(t) - \underline{x}(t)) + V^\top|\delta(t)| \\ & & +V^\top|BK|(I+\Gamma)\left|\int_{\sigma(t)}^t e^{A(t-\ell)}\delta(\ell)\mathrm{d}\ell\right| + V^\top\lambda(\Delta_t) \end{array} \tag{36}$$

for all $t \geq 0$, where the second inequality in (36) used the formula for $x(t) - w(t)$ in (15) and the bounds

$$\begin{array}{l} V^\top|BK(x(t_i) - x(t))| - V^\top|BK||e(t)| \leq V^\top|BK||x(t) - w(t)| \text{ and} \\ V^\top|BK|\Gamma|w(t)| \leq V^\top|BK|\Gamma|x(t)| + V^\top|BK|\Gamma|x(t) - w(t)| \end{array} \tag{37}$$

which follow from the triangle inequality and our choice of e in (7), and where the last inequality in (36) followed from the bound $|x(t)| \leq \overline{x}(t) - \underline{x}(t)$ from (33). Hence,

$$\begin{array}{rcl} \dot{U}(t) & \leq & -cV^\top(\overline{x}(t) - \underline{x}(t) + z(t)) + V^\top|BK|\Gamma(\overline{x}(t) - \underline{x}(t)) + V^\top\Delta(t) \\ & & +V^\top|BK|(I+\Gamma)\left|\int_{\sigma(t)}^t e^{A(t-\ell)}\delta(\ell)\mathrm{d}\ell\right| + V^\top\lambda(\Delta_t), \end{array} \tag{38}$$

by Assumption 2. Since the first part of the proof gave $z(t) > 0$ for all $t \geq 0$, we deduce that

$$\begin{array}{rcl} \dot{U}(t) & \leq & -cV^\top(\overline{x}(t) - \underline{x}(t) + z(t)) + V^\top|BK|\Gamma(\overline{x}(t) - \underline{x}(t) + z(t)) + V^\top\Delta(t) \\ & & +V^\top|BK|(I+\Gamma)\left|\int_{\sigma(t)}^t e^{A(t-\ell)}\delta(\ell)\mathrm{d}\ell\right| + V^\top\lambda(\Delta_t) \\ & = & (-cV^\top + V^\top|BK|\Gamma)(\overline{x}(t) - \underline{x}(t) + z(t)) \\ & & +V^\top\Delta(t) + V^\top|BK|(I+\Gamma)\left|\int_{\sigma(t)}^t e^{A(t-\ell)}\delta(\ell)\mathrm{d}\ell\right| + V^\top\lambda(\Delta_t) \end{array} \tag{39}$$

for all $t \geq 0$. From (4) and the fact that $\overline{x} - \underline{x}$ and z are nonnegative valued, we deduce that

$$\dot{U}(t) \leq -rU(\overline{x}(t), \underline{x}(t), z(t)) + V^\top\Delta(t) + V^\top|BK|(I+\Gamma)\left|\int_{\sigma(t)}^t e^{A(t-\ell)}\delta(\ell)\mathrm{d}\ell\right| + V^\top\lambda(\Delta_t) \tag{40}$$

for all $t \geq 0$. Since Zeno's phenomenon does not occur, we deduce from (40) and Assumption 2 that

$$\begin{array}{rcl} U(\overline{x}(t), \underline{x}(t), z(t)) & \leq & e^{-rt}U(\overline{x}(0), \underline{x}(0), z(0)) + \int_0^t e^{r(m-t)}[V^\top\Delta(m) + V^\top\lambda(\Delta_m)]\mathrm{d}m \\ & & +V^\top|BK|(I+\Gamma)\int_0^t e^{r(m-t)}\int_{(m-T)^+}^m \left|e^{A(m-\ell)}\right|\Delta(\ell)\mathrm{d}\ell\mathrm{d}m \\ & \leq & e^{-rt}U(\overline{x}(0), \underline{x}(0), z(0)) + \int_0^t e^{r(m-t)}V^\top\Delta(m)\mathrm{d}m \\ & & + \int_0^t e^{r(m-t)}V^\top|BK|\left[\sup_{s\in[0,\nu]}\left|\Omega^{-1}(s)\right| + I + 2\Gamma\right]\int_{(m-\nu)^+}^m \left|e^{A(m-\ell)}\right|\Delta(\ell)\mathrm{d}\ell\mathrm{d}m \\ & & +V^\top|BK|(I+\Gamma)\int_0^t e^{r(m-t)}\int_{(m-T)^+}^m \left|e^{A(m-\ell)}\right|\Delta(\ell)\mathrm{d}\ell\mathrm{d}m \end{array} \tag{41}$$

for all $t \geq 0$, by applying the integrating factor e^{rt} and the method of variation of parameters to the differential inequality in (40) and using the fact that our trigger rule from (7) implies that $t_{i+1} - t_i \leq T$ for all i. This provides a constant $k > 0$ such that

$$U(\overline{x}(t), \underline{x}(t), z(t)) \leq e^{-rt}U(\overline{x}(0), \underline{x}(0), z(0)) + k\sup_{m\in[0,t]}|\Delta(m)|. \tag{42}$$

Hence, the dynamics for $(\overline{x}(t) - \underline{x}(t), z(t))$ satisfy an exponential ISS inequality. Since we may assume that $\overline{x}(0) \leq 2|x(0)|$ and $\underline{x}(0) \geq -2|x(0)|$ and so also $0 \leq \overline{x}(0) - \underline{x}(0) \leq 4|x(0)|$, and since $z(t) \geq 0$ for all $t \geq 0$,

(33) allows us to conclude from the structure (34) of U.

3 Systems with Outputs

3.1 Statement of Result

We next generalize Theorem 1 from the previous section to cover more general systems of the form

$$\dot{x}(t) = Ax(t) + Bu(t) + \delta(t) \ \ , \ \ y(t) = Cx(t), \tag{43}$$

for known matrices $C \in \mathbb{R}^{q \times n}$ where δ satisfies the requirements from Section 2.1, by adding this analog of [31, Assumption 4] whose conditions can be easily checked, e.g., using methods of [31, Section 4.2], where we fix a value $T > \nu$ as before (but see Remark 3.1 below for motivation for this assumption, and Appendix A.2 below for ways to check this assumption, and for an alternative version using linear Lyapunov functions, and see Appendix A.3 for other generalizations where the output $y(t)$ also contains uncertainties):

Assumption 3 *There are a constant $\kappa_0 \in (0,1)$, a positive definite matrix $Q \in \mathbb{R}^{n \times n}$, and a matrix $L \in \mathbb{R}^{n \times q}$ such that*

$$e^{A^\top \ell}(I - LC)^\top Q(I - LC)e^{A\ell} \preceq \kappa_0 Q \tag{44}$$

holds for all $\ell \in [\nu, T]$.

We interconnect the system and triggering rule from Theorem 1 with a continuous-discrete observer. Letting Assumptions 1-3 hold and using the notation from above, fix a diagonal matrix $D \in \mathbb{R}^{n \times n}$ whose main diagonal entries are all positive, and a positive vector $z_0 \in \mathbb{R}^n$. We now consider

$$\left\{ \begin{array}{rcl} \dot{x}(t) & = & Ax(t) + BKw(\sigma(t)) + \delta(t) \ \text{ for all } \ t \geq 0 \\ \dot{w}(t) & = & Aw(t) + BKw(t_i) \ \text{ for all } \ t \in [t_i, t_{i+1}) \ \text{ and } \ i \in \mathbb{Z}_0 \\ w(t_i) & = & w(t_i^-) + L(y(t_i) - Cw(t_i^-)) \ \text{ for all } \ i \in \mathbb{N} \\ \dot{z}(t) & = & (R_H + N_H)z(t) - |BK|(|e(t)| - \Gamma|w(t)|) + \lambda(t) \ \text{ for all } \ t \geq 0, \ \text{ and } \ z(0) = z_0 \\ e(t) & = & w(t_i) - w(t) \ \text{ for all } \ t \in [t_i, t_{i+1}) \ \text{ and } \ i \in \mathbb{Z}_0 \\ t_{i+1} & = & \sup\{t \in [t_i, t_i + T] : z(t) - D|BK|(|e(t)| - \Gamma|w(t)|) + D\lambda(t) > 0\} \end{array} \right. \tag{45}$$

where $t_0 = 0$ and $w(0)$ is an initial estimate of $x(0)$, and where $\lambda(\Delta_t)$ from Theorem 1 has been replaced by

$$\begin{array}{rcl} \lambda(t) & = & |BK| \left[\sup\limits_{s \in [0,\nu]} \left|\Omega^{-1}(s)\right| + I + 2\Gamma \right] \int_{(t-\nu)^+}^t \left|e^{A(t-\ell)}\right| \Delta(\ell) \mathrm{d}\ell + \max\limits_{s \in [0,\nu]} J(s) \mathbf{1}_n \kappa_*^{\sigma(t)/(2T)} \sqrt{\frac{\lambda_{\max}}{\lambda_{\min}}} b_0 \\ & & + \max\limits_{s \in [0,\nu]} J(s) \mathbf{1}_n \sqrt{\frac{\kappa_* \kappa_{**}}{\lambda_{\min}(1-\kappa_*)}} \int_{-T}^0 ||e^{A\ell}|| \mathrm{d}\ell ||\Delta||_{[0,\sigma(t)]}, \end{array} \tag{46}$$

where $\mathbf{1}_n \in \mathbb{R}^n$ is a vector whose entries are all 1's, the constant κ_{**} and $J : [0, \nu] \to \mathbb{R}^{n \times n}$ are defined by

$$\kappa_{**} = ||Q|| + \tfrac{||Q||^2}{\epsilon_0 \lambda_{\min}} \ \text{ and } \ J(s) = |BK| \left(\left|\Omega^{-1}(s) \int_0^s e^{Am} \mathrm{d}m BK - I\right| + (I + 2\Gamma) \left|e^{As}\right| \right), \tag{47}$$

$\lambda_{\max} > 0$ and $\lambda_{\min} > 0$ are the largest and smallest eigenvalues of Q respectively, $b_0 \geq 0$ is chosen such that $||w(0) - x(0)|| \leq b_0$, $\kappa_* = (1 + \epsilon_0)\kappa_0$ where $\epsilon_0 \in (0,1)$ is chosen small enough such that $\kappa_* \in (0,1)$, and $\sigma(t) = \max\{t_i : i \geq 0 \ \text{ and } \ t_i \leq t\}$ is the largest t_i in $[0,t]$ for each $t \geq 0$ as before (but see Appendices A.1-A.2 below for alternative λ formulas, including one satisfying $\lim_{t \to +\infty} \lambda(t) = 0$ if $\lim_{t \to +\infty} \Delta(t) = 0$).

The motivation for, and implementation of, (45) are as follows. The purpose of the w dynamics in (45) is to estimate the unmeasured state values $x(t)$ using only the sampled values $y(t_i)$. The w dynamics is continuous-discrete, because it is a continuous time dynamics on the intervals $[t_i, t_{i+1})$ between trigger times t_i but changes value in a discrete way at the t_i's, using the third equation in (45). Such dynamics are called reset systems in the robotics literature, or jump dynamics, because their states are reset at discrete times t_i.

The $w(t)$ values are found in the following recursive way. We start with an initial estimate $w(0)$ of the initial state $x(0)$ of (43). Often, this initial estimate is chosen to be the zero vector, but we allow nonzero

$w(0)$'s for generality, and because in engineering applications, one generally has some information about the initial state, which can lead to a smaller upper bound b_0 for the initial observation error than $||x(0)||$, by picking $w(0)$ closer to $x(0)$ than the zero vector. Then, starting from $w(0)$, we solve the initial value problem consisting of the second equation in (45) with the choice $i = 0$ and the initial value $w(0)$, to solve for the $w(t)$ values on the half open interval $[0, t_1)$, where the first positive triggering time t_1 is computed using the last equation in (45) with the choice $i = 0$, where t_1 is computed in a way that is analogous to the way that t_1 was computed in Theorem 1. Then, we store the left limit value $w(t_1^-)$ for w at time t_1, which we insert into the special case of the third equation of (45) where $i = 1$, which provides the value of $w(t_1)$ using the available values $w(t_1^-)$ and $y(t_1)$. The left limit $w(t_1^-)$ exists because of the linear growth of the differential equation part of the w dynamics in the second equation of (45). Then we solve the initial value problem consisting of the second equation of (45) in the special case where $i = 1$ and the initial state $w(t_1)$, to solve for $w(t)$ on the interval $[t_1, t_2)$ and to compute the left limit $w(t_2^-)$ of w at t_2, where t_2 is found from the last equation of (45) in the special case where $i = 1$. Then, we can use the third equation of (45) with $i = 2$ to define the value of $w(t_2)$, using $w(t_2^-)$ and $y(t_2)$. Then we can argue recursively to get $w(t)$ and a continuous solution $x(t)$ for all $t \geq 0$ and all triggering times t_i, because as we will show in the proof of the next theorem, the Zeno phenomenon does not occur.

Moreover, $w(t_i^-) = q_i(t_i)$ for all $i \in \mathbb{N}$, where q_i is the solution of the initial value problem

$$\dot{q}_i(t) = Aq_i(t) + BKw(t_{i-1}), \;\; q_i(t_{i-1}) = w(t_{i-1}) \tag{48}$$

for all $i \in \mathbb{N}$, so the left limits $w(t_i^-)$ can be found by solving the initial value problems (48). Also, note that the control $u(t) = Kw(\sigma(t))$ in the x dynamics (45) is not the same as the control $u(t) = Kx(\sigma(t))$ from (7) in Theorem 1 even if δ is the zero function, because of the jumps in w as stipulated in the third equality in (45). Finally, the integral and maximized J values in (46) that were not in (8) can be calculated prior to implementing (45) (using the known values of ν and T), and so do not add any computational burden for the implementation. In terms of the notation above, our result for systems with outputs is:

Theorem 2 *Let Assumptions 1-3 hold. Set*

$$r_0 = \min\left\{\tfrac{r}{2}, -\tfrac{\ln(\kappa_*)}{4T}\right\}. \tag{49}$$

Then we can find positive constants c_1 and c_2 so that for all solutions $x : [0, +\infty) \to \mathbb{R}^n$ of (43) with the choices (45) and $u(t) = Kw(\sigma(t))$, we have

$$||x(t)|| \leq c_1 e^{-r_0 t}||(x(0), z_0, b_0)|| + c_2||\Delta||_{[0,t]} \tag{50}$$

for all $t \geq 0$. Also, $t_{i+1} - t_i \in [\nu, T]$ for all $i \in \mathbb{Z}_0$.

As in the case for systems without outputs from Theorem 1, the special case where there is no uncertainty δ ensures exponential convergence of $||x(t)||$ to the origin as $t \to +\infty$, by taking Δ to be the zero function.

Remark 3.1 Assumptions 1-2 are not at all restrictive, because (i) as noted, e.g., in [21], Assumption 1 can be satisfied after a change of coordinates when the pair (A, B) is controllable, and because controllability of a pair is generic, in the sense that almost all pairs are controllable because (as noted, e.g., in [35, p.97]) the set of all uncontrollable pairs constitute a set of Lebesgue measure zero when the pairs are viewed as points in Euclidean space of dimension $n^2 + np$ and because (ii) bounds on uncertainties as we have them in Assumption 2 are normally known in practice. The change of coordinates to transform a controllable pair into a new pair that satisfies Assumption 1 is a similarity transformation of pairs, as defined, e.g., in [35]. On the other hand, our Assumption 3 is less standard, and contrasts with significant works like [25] that were designed for linear systems with outputs under more standard conditions, e.g., controllability and detectability. Moreover, whereas [25] calls for using state measurements in the dynamic event-triggered dynamics (e.g., the dynamics of η in [25, Equation 7]), our dynamic event-triggering approach from (45) uses a dynamic that can be computed from sampled output values. In this sense, our method may offer the significant advantage of requiring less information from the system, and Assumption 3 is the price to pay to achieve this potential advantage. See our numerical simulations in Section 5 below where all of our assumptions are easily checked, and where in addition we illustrate how our method can beneficially increase

the lower bound on the inter-execution times $t_{i+1} - t_i$, in order to ensure a priori that trigger times do not occur too frequently.

3.2 Proof of Theorem 2

We explain the changes in the proof of Theorem 1 that are needed to prove Theorem 2. The proof has the same structure as the proof of Theorem 1, the first part of the proof is the same except with (46) replacing (8), and we change the second part as follows. In (11)-(12), we replace $\delta(m)$ in the integral by $\delta(m) + BK\tilde{x}(t_i)$ and subtract $\tilde{x}(t_i)$ from the right side (12), where $\tilde{x} = w - x$, because our new formula for e in (45) gives $e(t) = x(t_i) - w(t) + \tilde{x}(t_i)$ (instead of the formula $e(t) = x(t_i) - w(t)$ that we used in (7)) and $\dot{x}(t) = Ax(t) + BKx(t_i) + BK\tilde{x}(t_i) + \delta(t)$ for all $t \in [t_i, t_{i+1})$ and $i \in \mathbb{Z}_0$. Collecting terms, we then add

$$\left|\Omega^{-1}(t-t_i)\int_{t_i}^{t} e^{A(t-m)}\mathrm{d}mBK - I\right| |\tilde{x}(t_i)| \tag{51}$$

to the right sides of (13)-(14). Since $w(t_i)$ is no longer guaranteed to equal $x(t_i)$, we must change (15) to

$$x(t) - w(t) = \int_{t_i}^{t} e^{A(t-\ell)}\delta(\ell)\mathrm{d}\ell - e^{A(t-t_i)}\tilde{x}(t_i) \tag{52}$$

for all $i \in \mathbb{Z}_0$ and $t \in [t_i, t_{i+1})$, because $x(t_i) - w(t_i) = -\tilde{x}(t_i)$.

To get $t_{i+1} - t_i \in [\nu, T]$ for all $i \in \mathbb{Z}_0$ to rule out Zeno's phenomenon, we argue by contradiction. Suppose, for the sake of obtaining a contradiction, that there were an $i \in \mathbb{Z}_0$ such that $t_{i+1} - t_i < \nu$. Choose the minimal $i \in \mathbb{Z}_0$ such that $t_{i+1} - t_i < \nu$. Arguing as in the second part of the proof of Theorem 1 gives

$$\begin{aligned} |e(t)| - \Gamma|w(t)| \quad \leq \quad & \left|\Omega(t-t_i)^{-1}\int_{t_i}^{t} e^{A(t-m)}\delta(m)\mathrm{d}m\right| + (I+\Gamma)\left|\int_{t_i}^{t} e^{A(t-\ell)}\delta(\ell)\mathrm{d}\ell - e^{A(t-t_i)}\tilde{x}(t_i)\right| \\ & + \left|\Omega^{-1}(t-t_i)\int_{t_i}^{t} e^{A(t-m)}\mathrm{d}mBK - I\right| |\tilde{x}(t_i)| \quad \text{for all} \quad t \in [t_i, t_{i+1}), \end{aligned} \tag{53}$$

instead of (16). If $i = 0$, then

$$||\tilde{x}(t_i)|| = ||x(t_i) - w(t_i)|| \leq b_0 \leq \kappa_*^{\sigma(t_i)/2}\sqrt{\tfrac{\lambda_{\max}}{\lambda_{\min}}}b_0, \tag{54}$$

so we can assume in what follows that $i \geq 1$. Also, our choices of $\tilde{x} = w - x$ and (45), the continuity of $x(t)$, and the fact that $\dot{\tilde{x}}(t) = A\tilde{x}(t) - \delta(t)$ holds on (t_j, t_{j+1}) and $j \geq 0$ give

$$\tilde{x}(t_j) = (I - LC)\tilde{x}(t_j^-) = (I - LC)e^{(t_j - t_{j-1})A}\left(\tilde{x}(t_{j-1}) - \int_{t_{j-1}}^{t_j} e^{A(t_{j-1}-\ell)}\delta(\ell)\mathrm{d}\ell\right) \tag{55}$$

for all $j \in \{1, \ldots, i\}$ (by subtracting $x(t_j) = x(t_j^-)$ from both sides of the third equation of (45) and then applying the method of variation of parameters to the $\tilde{x}$ dynamics on $[t_{j-1}, t_j)$) and so also

$$||\tilde{x}(t_j)|| \leq \kappa_*^{j/2}\sqrt{\tfrac{\lambda_{\max}}{\lambda_{\min}}}||\tilde{x}(0)|| + \sqrt{\tfrac{\kappa_*\kappa_{**}}{\lambda_{\min}(1-\kappa_*)}}\int_{-T}^{0} ||e^{A\ell}||\mathrm{d}\ell||\Delta||_{[0,t_j]} \tag{56}$$

for all $j \in \{0, \ldots, i\}$. The inequality (56) follows by using Assumption 3 with $\ell = t_j - t_{j-1} \in [\nu, T]$ and the function $W(x) = x^\top Qx$ to get

$$\begin{aligned} \lambda_{\min}||\tilde{x}(t_j)||^2 \quad \leq \quad W(\tilde{x}(t_j)) \quad \leq \quad & \kappa_0 W(\tilde{x}(t_{j-1})) - 2\kappa_0\tilde{x}(t_{j-1})^\top Q\int_{t_{j-1}}^{t_j} e^{A(t_{j-1}-\ell)}\delta(\ell)\mathrm{d}\ell \\ & + \kappa_0\left[\int_{t_{j-1}}^{t_j} e^{A(t_{j-1}-\ell)}\delta(\ell)\mathrm{d}\ell\right]^\top Q\int_{t_{j-1}}^{t_j} e^{A(t_{j-1}-\ell)}\delta(\ell)\mathrm{d}\ell \\ \leq \quad & \kappa_* W(\tilde{x}(t_{j-1})) + \kappa_0\kappa_{**}\left(\int_{-T}^{0} ||e^{A\ell}||\mathrm{d}\ell||\Delta||_{[0,t_j]}\right)^2 \\ \leq \quad & \ldots \leq \kappa_*^j W(\tilde{x}(0)) + \tfrac{\kappa_*\kappa_{**}}{1-\kappa_*}\left(\int_{-T}^{0} ||e^{A\ell}||\mathrm{d}\ell||\Delta||_{[0,t_j]}\right)^2 \\ \leq \quad & \kappa_*^j\lambda_{\max}||\tilde{x}(0)||^2 + \tfrac{\kappa_*\kappa_{**}}{1-\kappa_*}\left(\int_{-T}^{0} ||e^{A\ell}||\mathrm{d}\ell||\Delta||_{[0,t_j]}\right)^2, \end{aligned} \tag{57}$$

where $\kappa_* \in (0,1)$ and κ_{**} are as defined in Section 3.1 above and the first inequality in (57) used (44) with

the choice $\ell = t_j - t_{j-1} \in [\nu, T]$ and (55), and the second inequality in (57) used Young's inequality to get

$$\begin{aligned} -2\kappa_0 \tilde{x}(t_{j-1})^\top Q \int_{t_{j-1}}^{t_j} e^{A(t_{j-1}-\ell)}\delta(\ell)\mathrm{d}\ell &\leq 2\kappa_0 ||\tilde{x}(t_{j-1})|| \left|\left|Q\int_{t_{j-1}}^{t_j} e^{A(t_{j-1}-\ell)}\delta(\ell)\mathrm{d}\ell\right|\right| \\ &\leq \kappa_0\epsilon_0\lambda_{\min}||\tilde{x}(t_{j-1})||^2 + \tfrac{\kappa_0}{\epsilon_0\lambda_{\min}}||Q||^2\left(\int_{-T}^0 ||e^{A\ell}||\mathrm{d}\ell||\Delta||_{[0,t_j]}\right)^2 \\ &\leq \kappa_0\epsilon_0 W(\tilde{x}(t_{j-1})) + \tfrac{\kappa_0}{\epsilon_0\lambda_{\min}}||Q||^2\left(\int_{-T}^0 ||e^{A\ell}||\mathrm{d}\ell||\Delta||_{[0,t_j]}\right)^2, \end{aligned} \tag{58}$$

and the last two inequalities in (57) used the geometric sum formula and the fact that $\kappa_* = (1+\epsilon_0)\kappa_0 \in (0,1)$ and the bound $W(\tilde{x}(0)) \leq \lambda_{\max}||\tilde{x}(0)||^2$, so (56) follows by dividing (57) through by $\lambda_{\min}$ and then using the subadditivity of the square root.

By our choice of J in (47), and because of the terms in (53) that were not present in (16), we must then subtract $J^\flat(t-t_i)|\tilde{x}(t_i)|$ from the right sides of (17)-(18) and from the left side of (19), where $J^\flat(s) = J(s) - |BK|\Gamma|e^{As}|$. The fact that (19) continues to hold with $J^\flat(t-t_i)|\tilde{x}(t_i)|$ subtracted from its left side follows from our formula (46) for $\lambda(t)$, (56), the fact that $|\tilde{x}(t_i)| \leq \mathbf{1}_n||\tilde{x}(t_i)||$ for all $i \in \mathbb{Z}_0$, and the fact that if t and j are such that $\sigma(t) = t_j$, then we have $Tj \geq \sigma(t)$, which gives

$$\kappa_*^{j/2} \leq \kappa_*^{\sigma(t)/(2T)} \tag{59}$$

since $\kappa_* \in (0,1)$. The rest of the second part is the same as that part of the proof of Theorem 1, except using (52) instead of (15), and with $DJ^\flat(t-t_i)|\tilde{x}(t_i)|$ added on the left side of (21), where the 2 was required in the formula for J in (47) because of the term in (52) that was not in (15). Hence, $t_{i+1} - t_i \in [\nu, T]$ for all i.

The third part is the same as that part of the proof of Theorem 1, except we change (26) to

$$\left\{\begin{array}{rcl} \dot{\overline{x}}(t) &=& R_H\overline{x}(t) - N_H\underline{x}(t) + (BK(w(\sigma(t)) - x(t)))^+ + \delta(t)^+ \\ \dot{\underline{x}}(t) &=& R_H\underline{x}(t) - N_H\overline{x}(t) - (BK(w(\sigma(t)) - x(t)))^- - \delta(t)^- \end{array}\right. \tag{60}$$

and use the fact that $\dot{x}(t) = (R_H - N_H)x(t) + BK(w(\sigma(t)) - x(t)) + \delta(t)$ for all $t \geq 0$. This lets us again conclude that (32)-(33) hold when (31) holds. The fourth part again uses U from (34), and the fact that $\dot{\overline{x}}(t) - \dot{\underline{x}}(t) = (R_H + N_H)(\overline{x}(t) - \underline{x}(t)) + |BK(w(\sigma(t)) - x(t))| + |\delta(t)|$ for all $t \geq 0$ to conclude that the time derivative of U along the solutions of the closed loop system from the statement of Theorem 2 satisfies

$$\begin{aligned} \dot{U}(t) &\leq -cV^\top(\overline{x}(t) - \underline{x}(t)) + V^\top|BK(w(\sigma(t)) - x(t))| - cV^\top z(t) - V^\top|BK|(|e(t)| - \Gamma|w(t)|) \\ &\quad + V^\top|\delta(t)| + V^\top\lambda(t) \\ &\leq -cV^\top(\overline{x}(t) - \underline{x}(t) + z(t)) + V^\top|BK|\Gamma|x(t)| + V^\top|\delta(t)| \\ &\quad + V^\top|BK|(\Gamma + I)\left|\int_{\sigma(t)}^t e^{A(t-\ell)}\delta(\ell)\mathrm{d}\ell\right| + V^\top\lambda(t) + V^\top|BK|(I+\Gamma)|e^{A(t-\sigma(t))}||\tilde{x}(\sigma(t))| \end{aligned} \tag{61}$$

and therefore also

$$\begin{aligned} \dot{U}(t) &\leq -cV^\top(\overline{x}(t) - \underline{x}(t) + z(t)) + V^\top|BK|\Gamma(\overline{x}(t) - \underline{x}(t) + z(t)) + V^\top|\delta(t)| \\ &\quad + V^\top|BK|(\Gamma + I)\left|\int_{\sigma(t)}^t e^{A(t-\ell)}\delta(\ell)\mathrm{d}\ell\right| + V^\top\lambda(t) + V^\top|BK|(I+\Gamma)|e^{A(t-\sigma(t))}||\tilde{x}(\sigma(t))| \end{aligned} \tag{62}$$

for all $t \geq 0$ (instead of (36)), where the second inequality in (61) follows from the bound $V^\top|BK(w(\sigma(t)) - x(t))| - V^\top|BK||e(t)| = V^\top|BK||w(\sigma(t)) - x(t)| - V^\top|BK||w(\sigma(t)) - w(t)| \leq V^\top|BK||x(t) - w(t)|$, (52), and the bound $V^\top|BK|\Gamma|w(t)| \leq V^\top|BK|\Gamma|x(t)| + V^\top|BK|\Gamma|x(t) - w(t)|$, and where (62) followed from (33) and the nonnegative valuedness of $z(t)$.

Then we obtain (38)-(40) except with $V^\sharp|\tilde{x}(\sigma(t))|$ added to the right sides of the three inequalities and with $\lambda(t)$ instead of $\lambda(\Delta_t)$, where $V^\sharp = V^\top|BK|(I+\Gamma)\sup_{\ell\in[0,T]}|e^{A\ell}|$. We can therefore use the nonnegative valuedness of $\overline{x} - \underline{x} + z$, our condition on r from (4), and our definition (46) of $\lambda(t)$ to find a constant $b_* > 0$ such that

$$\dot{U}(t) \leq -rU(\overline{x}(t), \underline{x}(t), z(t)) + b_*\left(||\Delta||_{[0,t]} + ||\tilde{x}(\sigma(t))|| + \kappa_*^{\sigma(t)/(2T)}b_0\right) \tag{63}$$

for all $t \geq 0$. Also, since we showed that $t_{i+1} - t_i \in [\nu, T]$ for all $i \in \mathbb{Z}_0$ in the second part of the proof, the

argument that produced (56) also gives

$$||\tilde{x}(\sigma(t))|| \leq \kappa_*^{\sigma(t)/(2T)} \sqrt{\tfrac{\lambda_{\max}}{\lambda_{\min}}} b_0 + \sqrt{\tfrac{\kappa_* \kappa_{**}}{\lambda_{\min}(1-\kappa_*)}} \int_{-T}^{0} ||e^{A\ell}|| \mathrm{d}\ell ||\Delta||_{[0,t]} \tag{64}$$

for all $t \geq 0$. By using (64) to upper bound $||\tilde{x}(\sigma(t))||$ in (63) and then collecting terms, we get

$$\begin{array}{rcl} \dot{U}(t) & \leq & -rU(\overline{x}(t), \underline{x}(t), z(t)) + b_* b_\alpha ||\Delta||_{[0,t]} + b_* b_\beta \kappa_*^{t/(2T)} b_0 \\ & \leq & -rU(\overline{x}(t), \underline{x}(t), z(t)) + b^\sharp \left(||\Delta||_{[0,t]} + b_0 \kappa_*^{t/(2T)} \right) \end{array} \tag{65}$$

for all $t \geq 0$, where $b^\sharp = b_* \max\{b_\alpha, b_\beta\}$, where

$$b_\alpha = 1 + \sqrt{\tfrac{\kappa_* \kappa_{**}}{\lambda_{\min}(1-\kappa_*)}} \int_{-T}^{0} ||e^{A\ell}|| \mathrm{d}\ell \ \text{ and } \ b_\beta = \kappa_*^{-1/2} \left(1 + \sqrt{\tfrac{\lambda_{\max}}{\lambda_{\min}}} \right), \tag{66}$$

using the bound $\sigma(t) \geq t - T$ to get

$$\kappa_*^{\sigma(t)/(2T)} \leq \kappa^{t/(2T)} \kappa_*^{-1/2} \tag{67}$$

(because $\kappa_* \in (0,1)$), to get the b_β formula.

By applying an integrating factor to apply the method of variation of parameters to (65) on the interval $[t/2, t]$ and then on the interval $[0, t/2]$, we obtain

$$\begin{array}{l} U(\overline{x}(t), \underline{x}(t), z(t)) \leq e^{-rt/2} U(\overline{x}(t/2), \underline{x}(t/2), z(t/2)) + \frac{b^\sharp}{r} \left(||\Delta||_{[0,t]} + b_0 e^{\ln(\kappa_*) t/(4T)} \right) \ \text{ and} \\ U(\overline{x}(t/2), \underline{x}(t/2), z(t/2)) \leq e^{-rt/2} U(\overline{x}(0), \underline{x}(0), z(0)) + \frac{b^\sharp}{r} \left(||\Delta||_{[0,t/2]} + b_0 \right) \end{array} \tag{68}$$

for all $t \geq 0$. By using the second inequality in (68) to upper bound the $U(\overline{x}(t/2), \underline{x}(t/2), z(t/2))$ in the first inequality in (68) and then collecting terms, we get

$$U(\overline{x}(t), \underline{x}(t), z(t)) \leq \left(1 + \tfrac{2b^\sharp}{r} \right) e^{-r_0 t} \big|\big| \big(U(\overline{x}(0), \underline{x}(0), z(0)), b_0 \big) \big|\big| + \tfrac{2b^\sharp}{r} ||\Delta||_{[0,t]} \tag{69}$$

for all $t \geq 0$, where $r_0 = \min\{r/2, -\ln(\kappa_*)/(4T)\}$. Then the final ISS estimate follows by assuming that $\overline{x}(0) \leq 2|x(0)|$ and $\underline{x}(0) \geq -2|x(0)|$, to use our condition (33) to conclude as before.

4 Comparison of Trigger Rules

When saying that one event-triggered control method outperforms another method, it is important to first decide which criteria to use to compare the performance of different triggering rules. As noted in [26], three criteria one can use to compare the performances of two event-triggered mechanisms are (i) determining which trigger rule produces a larger next trigger time t_{i+1}, when both trigger rules are used to control the same system starting from the same given time t_i and with the same initial state $x(t_i)$ used for both triggers at time t_i, i.e., which trigger rule triggers sooner, since then the one that triggers later may be advantageous, (ii) determining which trigger provides a larger lower bound on the inter-execution times, i.e., a larger lower bound on the infimum for the amounts of time $t_{i+1} - t_i$ between its trigger times, and (iii) other performance indices such as mean values or coefficient of variation of the inter-execution times. The first criterion is motivated by the fact that in applications where one wants to avoid unnecessarily frequent changes in control values, one may prefer the trigger rule that triggers later. The other criteria are motivated by the desire to keep the inter-execution times $t_{i+1} - t_i$ from becoming too small. In this section, we explain why our approach based on matrices of absolute values from our theorems above may offer advantages using the first criterion, compared with previous static event-triggering rules, and we review the necessary formulas for the lower bounds on the inter-execution times from [26]. In the next section, we illustrate how our new methods can be advantageous using other criteria and formulas from [26] that we review in this section.

As was the case in [26], our dynamic event triggering has the potential to reduce the number of triggering times compared with static event triggering methods, by triggering later than the static one, in the sense of [26]. To see how, let us denote the value t_{i+1} obtained by (7) with $\delta = 0$ by t_{i+1}^d if the value of the state at

time t_i were $x(t_i)$. Since $\delta = 0$, we have $w = x$, and we choose $\Delta = 0$. Let us denote by t_{i+1}^s the $(i+1)$st triggering time that is obtained by the static event trigger mechanism

$$\left\{ \begin{array}{rcl} \dot{x}(t) & = & Ax(t) + BKx(t_i) \\ e(t) & = & x(t_i) - x(t) \ \text{ for all } \ t \in [t_i, t_{i+1}) \\ t_{i+1} & = & \sup\{t \geq t_i : \Gamma|x(t)| - |e(t)| \geq 0\} \end{array} \right. \tag{70}$$

if the state at time t_i is $x(t_i)$. As in [26], we show now that $t_{i+1}^s \leq t_{i+1}^d$. To show this, we argue by contradiction. Suppose that $t_{i+1}^s > t_{i+1}^d$. Then (70) gives $\Gamma|x(t)| - |e(t)| \geq 0$ for all $t \in [t_i, t_{i+1}^d]$. Since $z(t) > 0$ for all $t \geq 0$, we deduce that

$$z(t) - D|BK|(|e(t)| - \Gamma|x(t)|) > 0 \tag{71}$$

for all $t \in [t_i, t_{i+1}^d]$. This contradicts the definition of t_{i+1}^d as a supremum and the right continuity of $e(t)$. As noted in [26, Remark 2.4], one cannot apply this result repeatedly to show that the dynamic approach always gives better results than the static one. However, in the next section, we illustrate how our new dynamic triggers can reduce the numbers of trigger times on given intervals compared with previous static and dynamic event triggering mechanisms.

For the second criterion, note that our lower bound ν on the inter-execution times for our dynamic event-triggered control is the largest available $\nu > 0$ such that $|\Omega^{-1}(s) - I| \leq \Gamma$ for all $s \in [0, \nu]$, where Ω and Γ satisfy the requirements from Section 2.1, and these requirements can be met for all controllable pairs (A, B) for a suitable choice of K in Section 2.1, after a change of coordinates; see Remark 3.1. By contrast, for the same class of systems, [26] used the usual Euclidean norm, and reported the lower bound for the inter-execution time, as follows. First, [26] found matrices $K \in \mathbb{R}^{p \times n}$, P_0, and Q_0, with P_0 and Q_0 being positive definite $n \times n$ matrices, such that

$$(A + BK)^\top P_0 + P_0(A + BK) = -Q_0, \tag{72}$$

and then used the dynamic extension

$$\dot{\eta}(t) = -\lambda\eta(t) + \bar{\sigma}x^\top(t)Q_0x(t) - 2x^\top(t)P_0BK\big(x(\sigma(t)) - x(t)\big), \ \ \eta(0) = \eta_0 \tag{73}$$

and the trigger times

$$t_{i+1} = \inf\left\{t \geq t_i : \eta(t) + \theta\big(\bar{\sigma}x^\top(t)Q_0x(t) - 2x^\top(t)P_0BK(x(\sigma(t)) - x(t^-))\big) \leq 0\right\} \tag{74}$$

with $t_0 = 0$, where the constants $\bar{\sigma} \in (0,1)$, $\lambda > 0$, $\theta > 0$, and $\eta_0 > 0$ are design parameters, and where $\sigma(t)$ is the largest trigger time on $[0, t]$ as before. Using the preceding notation, [26] then provided the following maximum lower bound on the inter-execution times, where we use the notation τ_0 to distinguish this lower bound from the lower bound ν that we obtained from Theorems 1-2 from the previous sections:

$$\tau_0 = \left\{ \begin{array}{ll} \displaystyle\int_0^1 \frac{1}{a\frac{p}{\bar{\sigma}q_0} + (a+b)s + b\frac{\bar{\sigma}q_0}{p}s^2}\mathrm{d}s, & \text{if } \ a \leq \lambda/2 \\ \displaystyle\int_0^1 \frac{1}{a\frac{p}{\bar{\sigma}q_0} + (a+b)s + b\frac{\bar{\sigma}q_0}{p}s^2 + \left(a - \frac{\lambda}{2}\right)(s^3 - s)}\mathrm{d}s, & \text{if } \ a > \lambda/2 \ \text{ and } \ \theta \leq 1/(2a - \lambda) \\ \displaystyle\int_0^1 \frac{1}{a\frac{p}{\bar{\sigma}q_0} + (a+b)s + b\frac{\bar{\sigma}q_0}{p}s^2 + \frac{1}{2\theta}(s^3 - s)}\mathrm{d}s, & \text{if } \ a > \lambda/2 \ \text{ and } \ \theta > 1/(2a - \lambda) \end{array} \right. \tag{75}$$

where $q_0 > 0$ is the smallest eigenvalue of Q_0, $p = 2||P_0BK||$, $a = ||A + BK||$, and $b = ||BK||$. Also, as noted in [26], the first case lower bound in (75) coincides with the lower bound in the static event-triggered case of [36], but the other lower bounds for the other two cases in (75) are strictly larger than the lower bound for the first case. Moreover, (75) is a continuous function of θ that is constant on $[0, 1/(2a - \lambda)]$, strictly decreasing on $[1/(2a - \lambda), +\infty)$ (since $s^3 - s < 0$ for all $s \in (0,1)$), and converges towards the static event-triggered lower bound on the inter-execution times (i.e., the first integral in (75)) as $\theta \to +\infty$. We turn next to our illustration of advantages of our methods, using some of the previous criteria and (75).

5 Application to BlueROV2 Marine Vehicle

We revisit a dynamics for the control of the depth and pitch degrees-of-freedom (or DOF) of an autonomous underwater vehicle (or AUV) that we studied in [20, 22], e.g., the BlueROV2 vehicle, which is widely used in environmental surveys such as the study of corals. As in [20, 22], we assume that the vehicle has a Doppler Velocity Logger (or DVL) for estimating its velocity. The DVL commonly experiences bottom lock, making it impractical to continuously change the control values. Hence, we show how our new dynamic event-triggered approach applies, and so we cover cases where only sampled measurements (instead of continuous measurements) are needed in the triggering rule, which were beyond the scope of [22] or other event-triggered studies of the dynamics that required continuous system measurements.

As noted in [37, Equation (9.28)], after linearization and assuming that the vehicle is neutrally buoyant, the linearized dynamics for the depth plane are given by

$$\begin{aligned}&(m - X_{\dot{w}(t)})\dot{w}(t) - (mx_g + Z_{\dot{q}})\dot{q}(t) - Z_w w(t) - (mU(t) + z_q)q(t) = Z_{\gamma_s} u_Z\\ &(mx_g + M_{\dot{w}}(t))\dot{w}(t) + (I_{yy} - M_{\dot{q}})\dot{q}(t) - M_w w(t) + (mx_g U - M_q)q(t) - M_\theta \theta = M_{\gamma_s} u_M\end{aligned} \tag{76}$$

whose parameter values were experimentally computed and presented in [37]. As in [22], we assume that the surge nominal velocity is $U = 0.1$m/s. The states represent the depth velocity w and the pitch velocity q, and the controls u_Z and u_M are the force and moment required to produce motion of the vehicle. Using the parameter values and controller from [37], the system (76) becomes $\dot{x}(t) = Ax(t) + Bu$ with

$$A = \begin{bmatrix} -0.387 & 0 \\ 0 & -1.8 \end{bmatrix} \text{ and } B = \begin{bmatrix} 0.038 \\ 1.5 \end{bmatrix}, \tag{77}$$

which are the A and B choices in [20]. Choosing

$$K = [-0.977852, -0.097546799] \tag{78}$$

provides the eigenvalues -1.94988 and -0.420595 for the matrix

$$A + BK = \begin{bmatrix} -0.424158 & -0.00370678 \\ -1.46678 & -1.94632 \end{bmatrix} \tag{79}$$

which satisfies our requirements from Assumption 1 with $H = A + BK$. To satisfy the requirements (3), (4), and (6) from Section 2.1, we chose $V = [2, 0.2]^\top$, $c = 3.9$, $r = 0.02$, $\nu = 0.72$, and

$$\Gamma = \begin{bmatrix} 0.90 & 0.012 \\ 1.36 & 0.9 \end{bmatrix}. \tag{80}$$

With the preceding choices, we carried out MATLAB simulations, first using the static event-triggered method from [20, Theorem 1] and then using the dynamic event-triggered control method from Theorem 1 from Section 2.2 with $D = I$, $\delta = 0$, and $T = 0.82$. We also evaluated the performance of the strategy when the Euclidean 2 norm is used instead of the absolute values in Theorem 1 and the one in [26]. We report our simulations in the figures below, for the initial states $(w_i(0), q_i(0))$ for the ith simulation for $i = 1, 2, 3$ that are indicated in Figure 1 below, with the model parameters kept the same in all of the simulations.

Averaged over the three sets of initial states, the static event-triggered method from [20] triggered 25 times while our dynamic trigger rule triggered 17 times on the same 20 second time horizon. Moreover, switching to the dynamic triggering rule did not introduce any substantial undershoots or overshoots, and the settling times were also not too adversely affected. This illustrates the benefits of using the dynamic event triggers from Theorem 1, namely, that they can reduce the numbers of triggering times to address bottom lock, while only requiring sampled measurements and also not adversely affecting the system performance. In our simulations, most of the trigger times occurred in the first 5 seconds, so we omit the trigger times in the figures to clearly highlight the control performance in terms of convergence properties.

Also, with the preceding parameter choices, we can satisfy the requirements of Theorem 2, e.g., with $Q = [Q_{ij}]$ with $Q_{11} = 5$ and $Q_{12} = Q_{21} = Q_{22} = 4$, $\kappa_0 = 0.8$, $C = [1, 1]$, $L = [0.7, 0.12]^\top$, $\nu = 0.72$, and

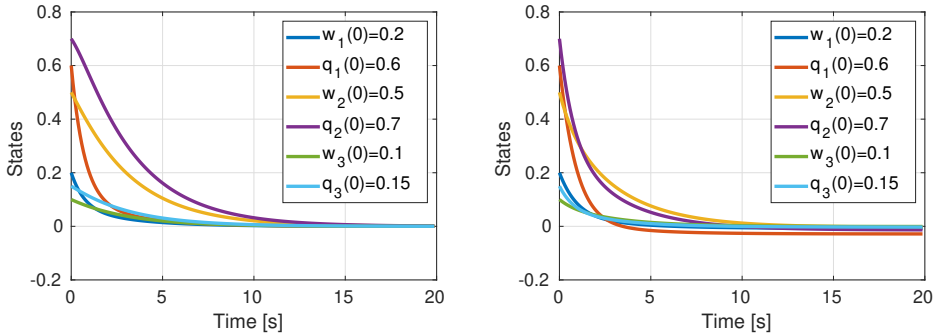

Figure 1: Comparison of Event-Triggered Controls: Static (Left Panel) and Dynamic (Right Panel)

any $T \in (0.72, 5]$, which correspond to only having sampled measurements of the sum of the state variables for the control and triggering rule. The simulation results can be seen in Figure 2, for the case when no disturbances are considered for the system and for the case when each of the components δ_i for δ were random disturbances that are uniformly sampled from the interval $(0.01, 0.08)$ at each time step. In the case with no disturbances, the controller was triggered on average 17 times over the three initial state vectors, while for the case when disturbances were considered, triggering was activated on average 33 times for the three initial state vectors. This improves on works such as [20], whose results for systems with outputs called for continuous measurements of the outputs in the triggering rule.

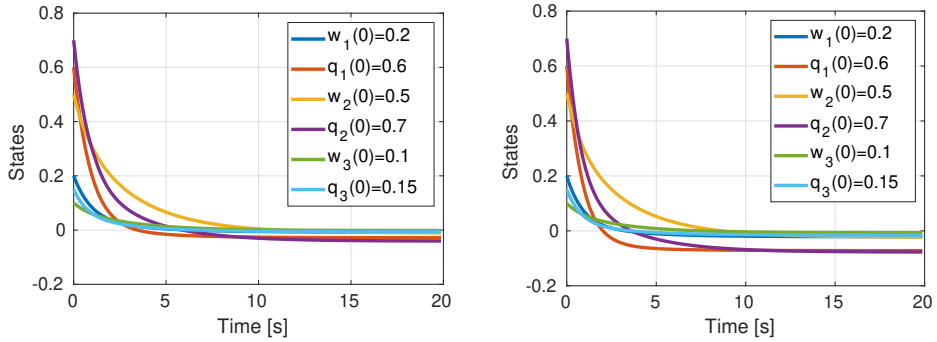

Figure 2: Simulation results for Theorem 2: No disturbances (Left) and with disturbances (Right)

In Figure 3, we present simulations using the dynamic control defined by (45) and (46), except with $|\cdot|$ replaced by the usual Euclidean norm $||\cdot||$, in order to demonstrate the possible advantage of using matrices of absolute values instead of the usual Euclidean norm. In this case all parameters are maintained as previously presented. When using the usual Euclidean norm, the controller was triggered on average 15 times averaged over the three initial state vectors when there were no disturbances, while for the case when disturbances were considered, triggering happened on average 44 times. These results are comparable with the case when the absolute value of matrices was used (instead of the Euclidean 2-norm) in Theorem 2, in terms of numbers of triggering times, but using the usual Euclidean norm produced larger overshoots or undershoots that were not present when we used our approach from (45)-(46). This demonstrates a potential advantage of using our approach based on interval observers and matrices of absolute values.

Lastly, we compared our approach from Theorem 1 with the approach presented in [26, Section III.A], as explained in Section 4 above. In order to isolate the effects of the different trigger rules, we kept all parameters the same in the simulations based on Theorem 1 and those that were based on [26, Section III.A], except for the trigger rules. We chose A and B from (77) and $K = [-0.977852, -0.097546799]$ as before and $Q_0 = I$ with $n = 2$, and then we solved the corresponding Riccati equation to obtain

$$P_0 = \begin{bmatrix} 1.73856 & -0.161868 \\ -0.161868 & 0.257203 \end{bmatrix}. \tag{81}$$

We then did simulations for different choices of the four design parameters. For instance, with $\sigma = 0.1$,

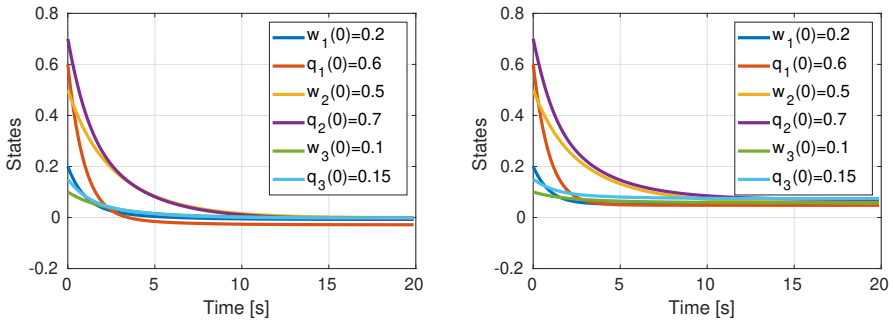

Figure 3: Simulation results for Theorem 2 when Euclidean norm is used: No disturbances (Left) and with disturbances (Right)

$\eta_0 = 1$, and $\lambda = \theta = 1$, the results can be seen in Figure 4.

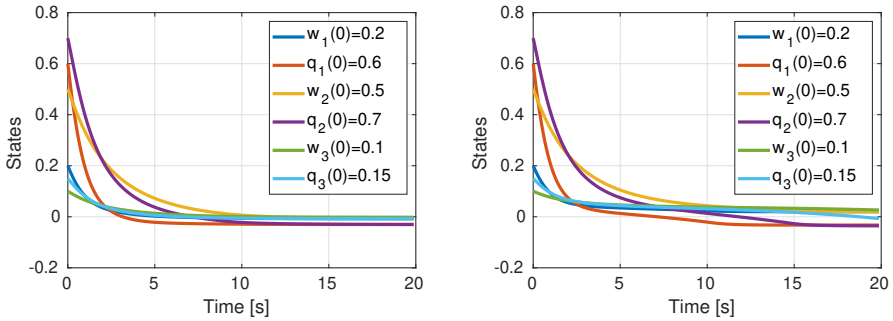

Figure 4: Simulation results for work presented in [26, Section III.A]: No disturbances (Left) and with disturbances (Right)

In this case, the number of triggers was on average 85 when no disturbances are present, and 207 when a disturbance is present in the system. We choose the disturbance as in our previous simulations above. We summarize results from all of our simulations in Table 1 below, where SSF-A indicates the simulation that used the static state feedback from [20] with matrices of absolute values, DSF-A (resp., DOF-A) means we used the dynamic state feedback from Theorem 1 (resp., Theorem 2) above with matrices of absolute values, DOF-E indicates that we used the method from Theorem 2 above except with matrices of absolute values replaced by the usual Euclidean norm, and DSF-E indicates a simulation that was done using the dynamic event-triggered rule from [26] using the values indicated above.

Event-Triggered Method	**Zero δ**	**Rand δ**
SSF-A from [20, Theorem 1]	25	-
DSF-A from Theorem 1	17	-
DOF-A from Theorem 2	17	33
DOF-E	15	44
DSF-E from [26, Sec. III.A]	85	207

Table 1: Average Numbers of Trigger Times in Figs. 1-4

In addition to the simulations pictured in Figs. 1-4, we ran simulations using the controls from Theorem 1 above and from [26, Section III.A] (with the same parameter values that we used to generate the comparisons in Table 1), for 30 different random initial state pairs $(w(0), q(0)) \in [0.2, 10] \times [-6.28, 0.89]$ without disturbances, and for 100 different random initial states in $[0.2, 10] \times [-6.28, 0.89]$ with disturbance amplitudes being random numbers on the interval $[0, 0.06]$, in order to examine the effects of increasing the size of the sample sets of initial states. For the simulations with the disturbances, the average number of triggers on the 20 second time horizon was 31.1 for the approach from Theorem 1, and 76.9 triggers for the approach from [26]. Also, for the simulations without disturbances, the approach from Theorem 1 produced 25.3 triggers

on average as compared with 94.4 triggers on average using the approach from [26]. We summarize these findings in Table 2 below.

Event-Triggered Method	**Zero δ**	**Rand δ**
DSF-A from Theorem 1	25.3	31.1
DSF-E from [26, Sec. III.A]	94.4	76.9

Table 2: Average Numbers of Triggers with Random Initial States

For the preceding examples, we know that our new trigger rules led to fewer trigger times in the cases indicated except for the DOF-E unperturbed case in Table 1, because all other parameters were kept the same in our comparisons, so all we changed were the triggering methods. This illustrates the potential advantages from using our method, which produced significantly fewer trigger times on the 20 second time horizon as compared with [26] in most cases, without adversely affecting control performance. Also, while the preceding simulations based on the method from [26] required continuous measurements $x(t)$ of the state, our approach only required sampled values $x(t_i)$ of the state, and so required less information for implementation.

The preceding cases and simulations compared triggered performance using criteria (iii) from Section 4, i.e., mean numbers of trigger times on an interval of a given length. In order to also compare our new trigger rules with state-of-the-art results such as [26], we next compare values of the lower bound τ_0 on the inter-execution times from (75) with the lower bound $\nu = 0.72$ that we obtained above. This will test our methods using the criterion (ii) from Section 4. The method in [26] called for choosing the design parameters λ and θ from Section 4 above. However, as a function of θ, the formula (75) for τ_0 shows that the maximal τ_0 occurs when $\theta = 1/(2a - \lambda)$, and that for this choice of θ, τ_0 is a decreasing function of λ. This motivates choosing $\lambda > 0$ smaller to get bigger τ_0 values. In Table 3, we show the values of τ_0 from (75) obtained for the choice $\theta = 1/(2a - \lambda)$ and for 81 combinations of the different possible values of $\lambda \in (0, 2a)$ (ranging from a lowest value of $\lambda = 0.1(2a) = 0.490207$ to a maximum value of $\lambda = 0.9(2a) = 4.41186$) and different possible values of $\sigma_0 \in (0, 1)$, where $a = ||A+BK||$ as before, the λ values are indicated by row headings, the σ_0 values are indicated by column headings, and we rounded our τ_0 values to the third decimal place to fit their values in Table 3. We computed the τ_0 values in Table 3 by using the numerical integration command `NIntegrate` in the Mathematica computer program to compute the second integral in (75). For instance, with the choices $\lambda = 0.5(2a)$ and $\sigma_0 = 0.6$, the second integral in (75) gave the value 0.199. In each of the 81 cases in Table 3, the A, B, K, P_0, and Q_0 values were chosen the same as for the simulation in Fig. 4.

	0.1	**0.2**	**0.3**	**0.4**	**0.5**	**0.6**	**0.7**	**0.8**	**0.9**
0.9(2a)	0.045	0.083	0.116	0.144	0.169	0.190	0.209	0.227	0.242
0.8(2a)	0.045	0.084	0.117	0.145	0.170	0.192	0.212	0.229	0.245
0.7(2a)	0.045	0.084	0.118	0.147	0.172	0.195	0.214	0.233	0.249
0.6(2a)	0.045	0.085	0.118	0.148	0.174	0.197	0.217	0.236	0.253
0.5(2a)	0.046	0.085	0.119	0.149	0.176	0.199	0.220	0.239	0.256
0.4(2a)	0.046	0.086	0.120	0.151	0.177	0.202	0.223	0.243	0.260
0.3(2a)	0.046	0.086	0.121	0.152	0.179	0.204	0.226	0.246	0.264
0.2(2a)	0.046	0.087	0.122	0.153	0.181	0.207	0.229	0.249	0.268
0.1(2a)	0.046	0.087	0.123	0.155	0.183	0.209	0.232	0.254	0.273

Table 3: Lower Bounds τ_0 on Inter-Execution Times for Values $\sigma_0 \in (0, 1)$ (Columns) and $\lambda \in (0, 2a)$ (Rows)

The preceding table indicates how the maximum lower bound τ_0 on the inter-execution times from [26] increases as $\sigma_0 \in (0, 1)$ increases towards 1 and as $\lambda \in (0, 2a)$ decreases towards 0, corresponding to moving from the upper left corner of the table to the lower right. However, the largest τ_0 values that we obtained from using (75) were significantly below the value $\nu = 0.72$ that we obtained for the lower bound for the inter-execution times using our positive systems approach, regardless of how small we chose λ in $(0, 2a)$ or how large we chose $\sigma \in (0, 1)$. For instance, with the choices $\lambda = 0.001(2a) = 0.00490207$ and $\sigma = 0.999$ and with A, B, K, P_0, and Q_0 chosen as we did for Table 3, formula (75) produced the value $\tau_0 = 0.295313$. This suggests that when using the linearized BlueROV2 dynamics with the other parameters specified above, it may be preferable to use our methods based on matrices of absolute values, instead of using the Euclidean 2-norm based event-triggered rules from [26], since our method ensures larger lower bounds on the inter-execution times $t_{i+1} - t_i$, and we found similar advantages using many other choices of Q_0.

6 Conclusion

We derived new event triggered control laws using the dynamic extension approach of [26] for the classes of systems in [20]. Key ingredients included our new triggering functions and our new interconnections of event-triggered dynamics with continuous-discrete observers. The continuous-discrete dynamics made it possible to compute the control values and trigger times from sampled values of an output, instead of requiring continuous measurements of the output. Our work also applies when the outputs contain uncertainties. Our application to a BlueROV2 dynamics illustrated how our new dynamic event triggering methods can reduce the numbers of triggering times on intervals on average, without substantial degradation of settling times and without producing undesirable overshoots or undershoots, as compared to dynamic event-triggered controls that used the usual Euclidean norm, and also as compared with static event-triggered controls that used interval observers and positive systems approaches. We also showed how our methods can lead to much larger lower bounds on the inter-execution times in the example, as compared with [26], when we substitute the earlier dynamic event-triggered control that was based on the usual Euclidean norm by our new event-triggered methods that were based on matrices of absolute values and interval observers but keep all other parameters the same. This is useful for knowing a priori that our new triggering rules can ensure larger time horizons between trigger rules, and thereby potentially lead to fewer trigger times on given intervals. This is a potential benefit for underwater vehicles that are prone to bottom lock, which precludes continuously changing the control values. Our event-triggered approach helps address the important need to reduce the numbers of times when control values change, to take communication and other resource constraints into account. A time-varying extension is expected. Our new approaches may also offer potential enhancement of state-of-the-art results on event-triggered communication applications [18] and consensus [19] by increasing the lower bounds on the inter-execution times. We hope to study these applications as well.

Appendix: Alternate Formulas for Triggering Function (46)

We show how we can replace the trigger function (46) in Theorem 2 by an alternative expression that satisfies the fading property that $\lim_{t\to+\infty}\lambda(t)=0$ when Δ from Assumption 2 also satisfies $\lim_{t\to+\infty}\Delta(t)=0$. Then we explain how to replace $\lambda(t)$ in (46) by a different expression that does not involve the Euclidean 2-norm, using a new discrete time interval observer for the dynamics for the error $\tilde{x}(t_i)=w(t_i)-x(t_i)$ between the state w of the continuous-discrete observer and the state x of the event-triggered system from Theorem 2.

A.1 Trigger Function with Fading Effect

A notable difference between the formula (8) for $\lambda(\Delta_t)$ from the triggering rule in Theorem 1 and the corresponding formula for $\lambda(t)$ in (46) for Theorem 2 is that, whereas $\lambda(\Delta_t)$ in Theorem 1 has the fading effect that $\lim_{t\to+\infty}\lambda(\Delta_t)=0$ when $\lim_{t\to+\infty}\Delta(t)=0$, we do not have $\lim_{t\to+\infty}\lambda(t)=0$ when $\lim_{t\to+\infty}\Delta(t)=0$ for the function λ in (46). However, we can prove a version of Theorem 2 in which the function λ in (46) is replaced by a new function $\lambda^\sharp$ that has this fading effect. We next show how this can be done.

To this end, first note that for any j such that $t_k-t_{k-1}\in[\nu,T]$ for all $k\in\{1,\dots,j\}$, the argument that led to (56) (except applied for all integers in $\{\lfloor j/2\rfloor,\dots,j\}$, and then to all integers in $\{0,\dots,\lfloor j/2\rfloor\}$) gives

$$\begin{aligned}
&||\tilde{x}(t_j)||\leq\kappa_*^{j/4}\sqrt{\tfrac{\lambda_{\max}}{\lambda_{\min}}}||\tilde{x}(t_{\lfloor j/2\rfloor})||+\sqrt{\tfrac{\kappa_*\kappa_{**}}{\lambda_{\min}(1-\kappa_*)}}\int_{-T}^{0}||e^{A\ell}||\mathrm{d}\ell||\Delta||_{[t_{\lfloor j/2\rfloor},t_j]}\ \text{and}\\
&||\tilde{x}(t_{\lfloor j/2\rfloor})||\leq\kappa_*^{\lfloor j/2\rfloor/2}\sqrt{\tfrac{\lambda_{\max}}{\lambda_{\min}}}||\tilde{x}(0)||+\sqrt{\tfrac{\kappa_*\kappa_{**}}{\lambda_{\min}(1-\kappa_*)}}\int_{-T}^{0}||e^{A\ell}||\mathrm{d}\ell||\Delta||_{[0,t_{\lfloor j/2\rfloor}]}
\end{aligned}\tag{A.1}$$

where $\lfloor\cdot\rfloor$ is the floor function. Using the second inequality in (A.1) to upper bound the $||\tilde{x}(t_{\lfloor j/2\rfloor})||$ on the right side of the first inequality in (A.1), and separately considering cases where j is even or odd, we obtain

$$\begin{aligned}
||\tilde{x}(t_j)|| \quad\leq\quad & \kappa_*^{j/2-1/4}\tfrac{\lambda_{\max}}{\lambda_{\min}}||\tilde{x}(0)||+\tfrac{\kappa_*^{j/4}}{\lambda_{\min}}\sqrt{\tfrac{\lambda_{\max}\kappa_*\kappa_{**}}{1-\kappa_*}}\int_{-T}^{0}||e^{A\ell}||\mathrm{d}\ell||\Delta||_{[0,t_{\lfloor j/2\rfloor}]}\\
&+\sqrt{\tfrac{\kappa_*\kappa_{**}}{\lambda_{\min}(1-\kappa_*)}}\int_{-T}^{0}||e^{A\ell}||\mathrm{d}\ell||\Delta||_{[t_{\lfloor j/2\rfloor},t_j]}.
\end{aligned}\tag{A.2}$$

Hence, if $i \in \mathbb{Z}_0$ is the first index such that $t_{i+1} - t_i < \nu$, then the reasoning that led to (46) and (59) imply that Theorem 2 remains true if we replace the definition of $\lambda(t)$ in (46) by

$$\begin{aligned}\lambda^\sharp(t) &= |BK| \left[\sup_{s\in[0,\nu]} \left|\Omega^{-1}(s)\right| + I + 2\Gamma \right] \int_{(t-\nu)^+}^t \left|e^{A(t-\ell)}\right| \Delta(\ell) \mathrm{d}\ell \\ &+ \max_{s\in[0,\nu]} J(s)\mathbf{1}_n \left(\kappa_*^{\sigma(t)/(2T)-1/4} \tfrac{\lambda_{\max}}{\lambda_{\min}} b_0 + \tfrac{\kappa_*^{\sigma(t)/(4T)}}{\lambda_{\min}} \sqrt{\tfrac{\lambda_{\max}\kappa_*\kappa_{**}}{1-\kappa_*}} \int_{-T}^0 ||e^{A\ell}|| \mathrm{d}\ell ||\Delta||_{[0,t_{\lfloor \sigma(t)/2 \rfloor}]} \right) \\ &+ \max_{s\in[0,\nu]} J(s)\mathbf{1}_n \sqrt{\tfrac{\kappa_*\kappa_{**}}{\lambda_{\min}(1-\kappa_*)}} \int_{-T}^0 ||e^{A\ell}|| \mathrm{d}\ell ||\Delta||_{[t_{\lfloor \sigma(t)/2 \rfloor}, t_{\sigma(t)}]},\end{aligned} \tag{A.3}$$

which enjoys the property that $\lim_{t\to+\infty} \lambda^\sharp(t) = 0$ when $\lim_{t\to+\infty} \Delta(t) = 0$, because $\kappa_* \in (0,1)$.

A.2 Use of Discrete Time Interval Observers

Using the well known Schur complement, it follows that for each positive definite matrix $Q \in \mathbb{R}^{n\times n}$ and each matrix $L \in \mathbb{R}^{n\times q}$ and each constant $\kappa_0 > 0$, the following two conditions are equivalent: (a) condition (44) from Assumption 3 is satisfied for all $\ell \in [\nu, T]$ and (b) the matrix

$$\begin{bmatrix} \kappa_0 Q & e^{A^\top \ell}(I - LC)^\top \\ (I - LC)e^{A\ell} & Q^{-1} \end{bmatrix} \tag{A.4}$$

is positive definite for each $\ell \in [\nu, T]$. This provides a useful alternative linear matrix inequality reformulation.

We can also prove a variant of Theorem 2 where we replace $\lambda(t)$ from (46) by an alternative expression that does not contain the Euclidean 2 norm, by building a discrete time interval observer for the dynamics

$$\tilde{x}(t_j) = P(t_j - t_{j-1})\tilde{x}(t_{j-1}) + P(t_j - t_{j-1})\mathcal{D}_j \tag{A.5}$$

for the error variable $\tilde{x} - w - x$ from (55) for any $j \in \{1, \ldots, i\}$, where the functions P and $\mathcal{D}_j$ in (A.5) are defined by

$$P(\ell) = (I - LC)e^{A\ell} \text{ and } \mathcal{D}_j = -\int_{t_{j-1}}^{t_j} e^{A(t_{j-1}-\ell)}\delta(\ell)\mathrm{d}\ell \tag{A.6}$$

and where as in the second part of the proof of Theorem 2, i is the smallest index such that $t_{i+1} - t_i < \nu$, so $t_j - t_{j-1} \in [\nu, T]$ for all $j \in \{1, \ldots, i\}$. This is done by replacing Assumption 3 by:

Assumption A.1 *There are a vector $W > 0$ in $\mathbb{R}^n$ and a constant $\kappa_0 \in (0,1)$ such that*

$$W^\top |P(\ell)| \le \kappa_0 W^\top \tag{A.7}$$

for all $\ell \in [\nu, T]$.

Since $|P(\ell)| \ge 0$, the preceding assumption means that $|P(\ell)|$ is Schur stable, with the additional requirement that W and κ_0 can be chosen independently of $\ell \in [\nu, T]$; see, e.g., [34, Lemma 2.7, p.79]. The assumption can therefore be interpreted to mean that $|P(0)|$ is Schur stable and that P is in some sense slowly time varying. To prove Theorem 2 with the preceding replacements, we first rewrite (A.5) as

$$\tilde{x}(t_j) = (P(t_j - t_{j-1}))^+ \tilde{x}(t_{j-1}) - (P(t_j - t_{j-1}))^- \tilde{x}(t_{j-1}) + P(t_j - t_{j-1})\mathcal{D}_j \tag{A.8}$$

and we use the discrete time interval observer

$$\begin{aligned}\overline{\tilde{x}}(t_j) &= (P(t_j - t_{j-1}))^+ \overline{\tilde{x}}(t_{j-1}) - (P(t_j - t_{j-1}))^- \underline{\tilde{x}}(t_{j-1}) + (P(t_j - t_{j-1})\mathcal{D}_j)^+ \\ \underline{\tilde{x}}(t_j) &= (P(t_j - t_{j-1}))^+ \underline{\tilde{x}}(t_{j-1}) - (P(t_j - t_{j-1}))^- \overline{\tilde{x}}(t_{j-1}) - (P(t_j - t_{j-1})\mathcal{D}_j)^-\end{aligned} \tag{A.9}$$

whose initial states are assumed to satisfy

$$\underline{\tilde{x}}(0) \le \tilde{x}(0) \le \overline{\tilde{x}}(0) \quad \text{and} \quad -2|\tilde{x}(0)| \le \underline{\tilde{x}}(0) \le 0 \le \overline{\tilde{x}}(0) \le 2|\tilde{x}(0)|. \tag{A.10}$$

By noting that the nonnegative orthant is forwardly invariant for the discrete time dynamics for $(\overline{\tilde{x}}, -\underline{\tilde{x}})$ and

for $(\overline{\tilde{x}} - \tilde{x}, \tilde{x} - \underline{\tilde{x}})$ (which follows from (A.8)-(A.9) by an induction argument on j), it follows that

$$\underline{\tilde{x}}(j) - \overline{\tilde{x}}(j) \leq \underline{\tilde{x}}(j) \leq \tilde{x}(j) \leq \overline{\tilde{x}}(j) \leq \overline{\tilde{x}}(j) - \underline{\tilde{x}}(j) \tag{A.11}$$

and therefore also

$$|\tilde{x}(j)| \leq \tilde{s}(j) \tag{A.12}$$

for all $j \in \{1, \ldots, i\}$, where $\tilde{s} = \overline{\tilde{x}} - \underline{\tilde{x}}$ satisfies

$$\tilde{s}(t_j) = |P(t_j - t_{j-1})|\tilde{s}(t_{j-1}) + |P(t_j - t_{j-1})\mathcal{D}_j| \tag{A.13}$$

for all $j \in \{1, \ldots, i\}$. Hence, Assumption A.1 gives

$$W^\top \tilde{s}(t_j) \leq \kappa_0 W^\top \tilde{s}(t_{j-1}) + \kappa_0 W^\top |\mathcal{D}_j| \tag{A.14}$$

for all $j \in \{1, \ldots, i\}$. Then we can argue inductively as in the second part of the proof of Theorem 2 and use our condition $\kappa_0 \in (0, 1)$ and the geometric sum formula to get

$$\begin{array}{rcccl} W^\top |\tilde{x}(t_j)| & \leq & W^\top \tilde{s}(t_j) & \leq & \kappa_0^j W^\top \tilde{s}(0) + \frac{\kappa_0}{1-\kappa_0} W^\top \int_{-T}^0 |e^{A\ell}| \mathrm{d}\ell |\Delta|_{[0,t_j]} \\ & & & \leq & 4\kappa_0^j W^\top |\tilde{x}(0)| + \frac{\kappa_0}{1-\kappa_0} W^\top \int_{-T}^0 |e^{A\ell}| \mathrm{d}\ell |\Delta|_{[0,t_j]} \end{array} \tag{A.15}$$

and so also

$$|\tilde{x}(t_j)| \leq \begin{bmatrix} \frac{1}{w_1} W^\top \\ \vdots \\ \frac{1}{w_n} W^\top \end{bmatrix} \left(4\kappa_0^j |\tilde{x}(0)| + \frac{\kappa_0}{1-\kappa_0} \int_{-T}^0 |e^{A\ell}| \mathrm{d}\ell |\Delta|_{[0,t_j]} \right) \tag{A.16}$$

for all $j \in \{1, \ldots, i\}$, by using the bound

$$w_i |\tilde{x}_i(t_j)| \leq W^\top |\tilde{x}(t_j)| \tag{A.17}$$

where $\tilde{x}_i(t_j)$ is the ith component of $\tilde{x}(t_j)$ for $i = 1, \ldots, n$ and separately considering the n components of $|\tilde{x}(t_j)|$, where w_i is the ith component of W for $i = 1, \ldots, n$, and where the third inequality in (A.15) followed from our initial conditions in (A.10). Then the reasoning that led to (46) implies that Theorem 2 remains true if we replace Assumption 3 by Assumption A.1 and if we replace the function $\lambda(t)$ in (46) by

$$\begin{array}{rcl} \lambda(t) & = & |BK| \left[\sup_{s \in [0,\nu]} \left| \Omega^{-1}(s) \right| + I + 2\Gamma \right] \int_{(t-\nu)^+}^t \left| e^{A(t-\ell)} \right| \Delta(\ell) \mathrm{d}\ell \\ & & + \max_{s \in [0,\nu]} J(s) \begin{bmatrix} \frac{1}{w_1} W^\top \\ \vdots \\ \frac{1}{w_n} W^\top \end{bmatrix} \left(4\kappa_0^{\sigma(t)/T} B_0 + \frac{\kappa_0}{1-\kappa_0} \int_{-T}^0 |e^{A\ell}| \mathrm{d}\ell |\Delta|_{[0,\sigma(t)]} \right) \end{array} \tag{A.18}$$

where $B_0 \in \mathbb{R}^n$ is any vector such that $|\tilde{x}(0)| \leq B_0$, which is expressed without using the Euclidean 2 norm.

A.3 Uncertainties in Measurements

Under our Assumptions 1-3, we can generalize Theorem 2 to cases where the measurement is instead

$$y(t) = Cx(t) + \delta_0(t) \tag{A.19}$$

for an unknown piecewise continuous function δ_0 that admits a known continuous function Δ_0 such that

$$|\delta_0(t)| \leq \Delta_0(t) \tag{A.20}$$

for all $t \geq 0$, by instead picking $\epsilon_0 \in (0, 1)$ such that $(1 + 1.5\epsilon_0)\kappa_0 \in (0, 1)$ (where the existence of such a constant $\epsilon_0 \in (0, 1)$ follows from the fact that the constant κ_0 as introduced in Assumption 3 was chosen

to satisfy $\kappa_0 \in (0,1)$, by choosing a small enough constant $\epsilon_0 > 0$), and then redefining κ_* and $\lambda(t)$ from Theorem 2 to be $\kappa_* = (1+1.5\epsilon_0)\kappa_0$ and

$$\begin{aligned}\lambda(t) &= |BK| \left[\sup_{s\in[0,\nu]} \left|\Omega^{-1}(s)\right| + I + 2\Gamma \right] \int_{(t-\nu)^+}^{t} \left|e^{A(t-\ell)}\right| \Delta(\ell)\mathrm{d}\ell + \max_{s\in[0,\nu]} J(s)\mathbf{1}_n \kappa_*^{\sigma(t)/(2T)} \sqrt{\tfrac{\lambda_{\max}}{\lambda_{\min}}} b_0 \\ &+ \max_{s\in[0,\nu]} J(s)\mathbf{1}_n \sqrt{\tfrac{\kappa_*\kappa_{**}}{\lambda_{\min}(1-\kappa_*)}} \int_{-T}^{0} ||e^{A\ell}||\mathrm{d}\ell\, ||\Delta||_{[0,\sigma(t)]} \\ &+ \max_{s\in[0,\nu]} J(s)\mathbf{1}_n \tfrac{1}{\sqrt{\lambda_{\min}(1-\kappa_*)}} \left[L_a ||\Delta_0||_{[0,t]}^2 + L_b \int_{-T}^{0} ||e^{A\ell}||\mathrm{d}\ell\, ||\Delta||_{[0,t]} ||\Delta_0||_{[0,t]} \right]^{1/2},\end{aligned} \tag{A.21}$$

respectively, where

$$L_a = \tfrac{L_b^2}{2\lambda_{\min}\kappa_0\epsilon_0} + ||L^\top Q L|| \text{ and } L_b = 2||I-LC|| \sup_{\ell\in[\nu,T]} ||e^{\ell A}||\, ||QL|| \tag{A.22}$$

and where the other notation is the same as what we used for Theorem 2. To obtain the preceding new formula for λ when the output is (A.19), we indicate the changes that are needed in the proof of Theorem 2.

The first and second parts of the proof remain the same, except (55) must be changed to

$$\tilde{x}(t_j) = (I-LC)\tilde{x}(t_j^-) + L\delta_0(t_j) = (I-LC)e^{(t_j-t_{j-1})A}\left(\tilde{x}(t_{j-1}) - \int_{t_{j-1}}^{t_j} e^{A(t_{j-1}-\ell)}\delta(\ell)\mathrm{d}\ell\right) + L\delta_0(t_j) \tag{A.23}$$

for all $j \in \{1,\ldots,i\}$, because the added disturbance δ_0 on the output $y(t) = Cx(t) + \delta_0(t)$ produces the new formula

$$w(t_j) = w(t_j^-) + L(Cx(t) - Cw(t_j^-)) + L\delta_0(t_j) \tag{A.24}$$

and because $\tilde{x} = w - x$. Also, since the formula $\dot{\tilde{x}}(t) = A\tilde{x}(t) - \delta(t)$ continues to hold for all $t \in (t_j, t_{j+1})$ and all $j \geq 0$, the lower bound

$$\lambda_{\min}||\tilde{x}(t_{j-1})||^2 \leq W(\tilde{x}(t_{j-1})) \tag{A.25}$$

and the bound (A.20) give

$$\begin{aligned}&2\left[(I-LC)\tilde{x}(t_j^-)\right]^\top QL\delta_0(t_j) \\ &\leq 2||I-LC|| \sup_{\ell\in[\nu,T]} ||e^{\ell A}|| \left(||\tilde{x}(t_{j-1})|| + \int_{-T}^{0} ||e^{A\ell}||\mathrm{d}\ell\, ||\Delta||_{[0,t_j]}\right) ||QL||\, ||\delta_0(t_j)|| \\ &= L_b \left(||\tilde{x}(t_{j-1})|| + \int_{-T}^{0} ||e^{A\ell}||\mathrm{d}\ell\, ||\Delta||_{[0,t_j]}\right) ||\delta_0(t_j)|| \\ &\leq \left(\sqrt{\epsilon_0\lambda_{\min}\kappa_0}||\tilde{x}(t_{j-1})||\right) \left(\tfrac{L_b}{\sqrt{\epsilon_0\lambda_{\min}\kappa_0}}||\Delta_0(t_j)||\right) + L_b \int_{-T}^{0} ||e^{A\ell}||\mathrm{d}\ell\, ||\Delta||_{[0,t_j]} ||\Delta_0(t_j)|| \\ &\leq \tfrac{\epsilon_0\kappa_0}{2} W(\tilde{x}(t_{j-1})) + \tfrac{L_b^2}{2\lambda_{\min}\kappa_0\epsilon_0}||\Delta_0(t_j)||^2 + L_b \int_{-T}^{0} ||e^{A\ell}||\mathrm{d}\ell\, ||\Delta||_{[0,t_j]} ||\Delta_0(t_j)||,\end{aligned} \tag{A.26}$$

where L_b was defined in (A.22), so and our choice of L_a in (A.22) gives

$$\begin{aligned}&2\left[(I-LC)\tilde{x}(t_j^-)\right]^\top QL\delta_0(t_j) + \left[L\delta_0(t_j)\right]^\top QL\delta_0(t_j) \\ &\leq \tfrac{\epsilon_0\kappa_0}{2} W(\tilde{x}(t_{j-1})) + L_a||\Delta_0(t_j)||^2 + L_b \int_{-T}^{0} ||e^{A\ell}||\mathrm{d}\ell\, ||\Delta||_{[0,t_j]} ||\Delta_0(t_j)||\end{aligned} \tag{A.27}$$

where the last inequality in (A.26) used the triangle inequality and (A.25). Hence, using the first equality in (A.23), it follows that the argument that gave (57) gives

$$\begin{aligned}\lambda_{\min}||\tilde{x}(t_j)||^2 \;\leq\; W(\tilde{x}(t_j)) \;\leq\; &\kappa_0 W(\tilde{x}(t_{j-1})) - 2\kappa_0 \tilde{x}(t_{j-1})^\top Q \int_{t_{j-1}}^{t_j} e^{A(t_{j-1}-\ell)}\delta(\ell)\mathrm{d}\ell \\ &+ \kappa_0 \left[\int_{t_{j-1}}^{t_j} e^{A(t_{j-1}-\ell)}\delta(\ell)\mathrm{d}\ell\right]^\top Q \int_{t_{j-1}}^{t_j} e^{A(t_{j-1}-\ell)}\delta(\ell)\mathrm{d}\ell \\ &+ 2\left[(I-LC)\tilde{x}(t_j^-)\right]^\top QL\delta_0(t_j) + \left[L\delta_0(t_j)\right]^\top QL\delta_0(t_j)\end{aligned} \tag{A.28}$$

and therefore also

$$\begin{aligned}
\lambda_{\min}||\tilde{x}(t_j)||^2 \;\leq\; W(\tilde{x}(t_j)) \;&\leq\; \kappa_* W(\tilde{x}(t_{j-1})) + \kappa_0\kappa_{**}\left(\textstyle\int_{-T}^{0}||e^{A\ell}||\mathrm{d}\ell||\Delta||_{[0,t_j]}\right)^2 \\
&\quad + L_a||\Delta_0(t_j)||^2 + L_b\textstyle\int_{-T}^{0}||e^{A\ell}||\mathrm{d}\ell||\Delta||_{[0,t_j]}||\Delta_0(t_j)|| \\
&\leq\; \ldots \leq \kappa_*^j W(\tilde{x}(0)) + \tfrac{\kappa_*\kappa_{**}}{1-\kappa_*}\left(\textstyle\int_{-T}^{0}||e^{A\ell}||\mathrm{d}\ell||\Delta||_{[0,t_j]}\right)^2 \\
&\quad + \tfrac{1}{1-\kappa_*}\left(L_a||\Delta_0||^2_{[0,t_j]} + L_b\textstyle\int_{-T}^{0}||e^{A\ell}||\mathrm{d}\ell||\Delta||_{[0,t_j]}||\Delta_0||_{[0,t_j]}\right) \\
&\leq\; \kappa_*^j\lambda_{\max}||\tilde{x}(0)||^2 + \tfrac{\kappa_*\kappa_{**}}{1-\kappa_*}\left(\textstyle\int_{-T}^{0}||e^{A\ell}||\mathrm{d}\ell||\Delta||_{[0,t_j]}\right)^2 \\
&\quad + \tfrac{1}{1-\kappa_*}\left(L_a||\Delta_0||^2_{[0,t_j]} + L_b\textstyle\int_{-T}^{0}||e^{A\ell}||\mathrm{d}\ell||\Delta||_{[0,t_j]}||\Delta_0||_{[0,t_j]}\right),
\end{aligned} \tag{A.29}$$

where the second inequality in (A.29) used (A.27), and where the third inequality in (A.29) used the geometric sum formula and the fact that $\epsilon_0 \in (0,1)$ was chosen such that our constant $\kappa_* = (1+1.5\epsilon_0)\kappa_0$ satisfies $\kappa_* \in (0,1)$, which allowed us to incorporate the effects of the first right side term in (A.27) into the $\kappa_* W(\tilde{x}(t_{j-1}))$ in (A.29). Therefore, instead of (56), we can divide (A.29) through by $\lambda_{\min}$ and then use the subadditivity of the square root to obtain the bound

$$\begin{aligned}
||\tilde{x}(t_j)|| \;&\leq\; \kappa_*^{j/2}\sqrt{\tfrac{\lambda_{\max}}{\lambda_{\min}}}||\tilde{x}(0)|| + \sqrt{\tfrac{\kappa_*\kappa_{**}}{\lambda_{\min}(1-\kappa_*)}}\textstyle\int_{-T}^{0}||e^{A\ell}||\mathrm{d}\ell||\Delta||_{[0,t_j]} \\
&\quad + \tfrac{1}{\sqrt{\lambda_{\min}(1-\kappa_*)}}\left[L_a||\Delta_0||^2_{[0,t_j]} + L_b\textstyle\int_{-T}^{0}||e^{A\ell}||\mathrm{d}\ell||\Delta||_{[0,t_j]}||\Delta_0||_{[0,t_j]}\right]^{1/2}.
\end{aligned} \tag{A.30}$$

Then we use (A.30) instead of (56) to bound the $||\tilde{x}(t_i)||$ terms in the remainder of the proof of Theorem 2. This produces the added terms in the formula (A.21) for λ that were not present in (46). Then the statement of Theorem 2 remains true, except with Δ in the final stability estimate replaced by (Δ, Δ_0).

References

[1] D. Borgers, V. Dolk, and W. Heemels, "Riccati-based design of event-triggered controllers for linear systems with delays," *IEEE Transactions on Automatic Control*, vol. 63, no. 1, pp. 174–188, 2018.

[2] A. Borri and P. Pepe, "Event-triggered control of nonlinear systems with time-varying state delays," *IEEE Transactions on Automatic Control*, vol. 66, no. 6, pp. 2846–2853, 2021.

[3] M. Di Ferdinando, S. Di Gennaro, A. Borri, G. Pola, and P. Pepe, "On the robustification of digital event-based stabilizers for nonlinear time-delay systems," *Nonlinear Analysis: Hybrid Systems*, vol. 52, no. 101463, 2024.

[4] L. Ding, K. Hashimoto, and S. Takai, "Synthesis of event-triggered controllers for SIRS epidemic models," *Nonlinear Analysis: Hybrid Systems*, vol. 51, no. 101437, 2024.

[5] V. Dolk, J. Ploeg, and W. Heemels, "Event-triggered control for string-stable vehicle platooning," *IEEE Transactions on Intelligent Transportation Systems*, vol. 18, no. 12, pp. 3486–3500, 2017.

[6] X. He, Y. Xing, J. Wu, and K. Johansson, "Event-triggered distributed estimation with decaying communication rate," *SIAM Journal on Control and Optimization*, vol. 60, no. 2, pp. 992–1017, 2022.

[7] W. Heemels, K. Johansson, and P. Tabuada, "An introduction to event-triggered and self-triggered control," in *Proceedings of the 51st IEEE Conference on Decision and Control*, 2012, pp. 3270–3285.

[8] C. Nowzari, E. Garcia, and J. Cortes, "Event-triggered communication and control of networked systems for multi-agent consensus," *Automatica*, vol. 105, pp. 1–27, 2019.

[9] P. Ong and J. Cortes, "Performance-barrier-based event-triggered control with applications to network systems," *IEEE Transactions on Automatic Control*, 2024, to appear, 15 pages, http://dx.doi.org/10.1109/TAC.2023.3318193.

[10] E. Petri, R. Postoyan, D. Astolfi, D. Nesic, and W. Heemels, "Decentralized event-triggered estimation of nonlinear systems," *Automatica*, vol. 160, no. 111414, 2024.

[11] Y. Xu, A. Seuret, K. Liu, and S. Chai, "Aperiodic dynamic event-triggered control for linear systems: A looped-functional approach," *Nonlinear Analysis: Hybrid Systems*, vol. 52, no. 101444, 2024.

[12] Q. Voortman, D. Efimov, A. Pogromsky, J.-P. Richard, and H. Nijmeijer, "Remote state estimation of steered systems with limited communications: an event-triggered approach," *IEEE Transactions on Automatic Control*, 2024, to appear, 15 pages, http://dx.doi.org/10.1109/TAC.2023.3318792.

[13] R. Zhang and J. Huang, "Event-triggered output-based adaptive distributed observer over jointly connected networks and its application," *Nonlinear Analysis: Hybrid Systems*, vol. 50, no. 101415, 2023.

[14] J. Zhang, T. Raissi, Q. Li, and D. Wu, "Distributed adaptive event-triggered fault detection filter of positive semi-Markovian jump systems," *Nonlinear Analysis: Hybrid Systems*, vol. 51, no. 101441, 2024.

[15] A. Maass, W. Wang, D. Nesic, R. Postoyan, and W. Heemels, "Event-triggered control through the eyes of a hybrid small-gain theorem," *IEEE Transactions on Automatic Control*, vol. 68, no. 10, pp. 5906–5921, 2023.

[16] C. De Persis, R. Postoyan, and P. Tesi, "Event-triggered control from data," *IEEE Transactions on Automatic Control*, 2024, to appear, https://doi.org/10.1109/TAC.2023.3335002.

[17] K. Scheres, R. Postoyan, and W. Heemels, "Robustifying event-triggered control to measurement noise," *Automatica*, vol. 159, no. 111305, 2024.

[18] V. Varma, R. Postoyan, D. Quevedo, and I.-C. Morarescu, "Event-triggered transmission policies for nonlinear control systems over erasure channels," *IEEE Control Systems Letters*, vol. 7, pp. 2113–2118, 2023.

[19] D. Antunes, D. Meister, T. Namerikawa, F. Allgöwer, and W. Heemels, "Consistent event-triggered consensus on complete graphs," in *Proceedings of the 62nd IEEE Conference on Decision and Control*, 2023, pp. 3911–3916.

[20] F. Mazenc, M. Malisoff, C. Barbalata, and Z.-P. Jiang, "Event-triggered control using a positive systems approach," *European Journal of Control*, vol. 62, pp. 63–68, 2021.

[21] ——, "Event-triggered control for linear time-varying systems using a positive systems approach," *Systems & Control Letters*, vol. 161, no. 105131, 2022.

[22] ——, "Event-triggered control for discrete-time systems using a positive systems approach," *IEEE Control Systems Letters*, vol. 6, pp. 1843–1848, 2022.

[23] F. Mazenc, M. Malisoff, and C. Barbalata, "Event-triggered control for continuous-time linear systems with a delay in the input," *Systems & Control Letters*, vol. 159, no. 105075, 2022.

[24] ——, "Event-triggered prediction-based delay compensation approach," *IEEE Control Systems Letters*, vol. 6, pp. 2515–2520, 2022.

[25] V. Dolk, D. Borgers, and W. Heemels, "Dynamic event-triggered control: Tradeoffs between transmission intervals and performance," in *Proceedings of the 53rd IEEE Conference on Decision and Control*, 2014, pp. 2764–2769.

[26] A. Girard, "Dynamic triggering mechanisms for event-triggered control," *IEEE Transactions on Automatic Control*, vol. 60, no. 7, pp. 1992–1997, 2015.

[27] Y. Yang, K. Vamvoudakis, H. Ferraz, and H. Modares, "Dynamic intermittent Q-learning for systems with reduced bandwidth," in *Proceedings of the IEEE Conference on Decision and Control*, 2018, pp. 924–931.

[28] J.-L. Gouzé, A. Rapaport, and M. Hadj-Sadok, "Interval observers for uncertain biological systems," *Ecological Modelling*, vol. 133, no. 1, pp. 45–56, 2000.

[29] V. Dolk, D. Borgers, and W. Heemels, "Output-based and decentralized dynamic event-triggered control with guaranteed Lp-gain performance and zeno-freeness," *IEEE Transactions on Automatic Control*, vol. 62, no. 1, pp. 34–49, 2016.

[30] X. Ge, Q.-L. Han, X.-M. Zhang, and D. Ding, "Dynamic event-triggered control and estimation: A survey," *International Journal of Automation and Computing*, vol. 18, no. 6, pp. 857–886, 2021.

[31] F. Mazenc, V. Andrieu, and M. Malisoff, "Design of continuous–discrete observers for time-varying nonlinear systems," *Automatica*, vol. 57, pp. 135–144, 2015.

[32] H. Khalil, *Nonlinear Systems, Third Edition.* Engelwood Cliffs, NJ: Prentice Hall, 2002.

[33] E. Sontag, "Input to state stability: Basic concepts and results," in *Nonlinear and Optimal Control Theory*, P. Nistri and G. Stefani, Eds. Berlin, Germany: Springer, 2008, pp. 163–220.

[34] W. Haddad, V. Chellaboina, and Q. Hui, *Nonnegative and Compartmental Systems*. Princeton, NJ: Princeton University Press, 2009.

[35] E. Sontag, *Mathematical Control Theory, Second Edition*. New York: Springer, 1998.

[36] P. Tabuada, "Event-triggered real-time scheduling of stabilizing control tasks," *IEEE Transactions on Automatic Control*, vol. 52, no. 9, pp. 1680–1685, 2007.

[37] T. Prestero, *Verification of a Six-Degree of Freedom Simulation Model for the REMUS Autonomous Underwater Vehicle*. Cambridge, MA: MS Thesis, MIT, 2001.